Chapter II
Thiadiazole derivatives having azomethine linkages

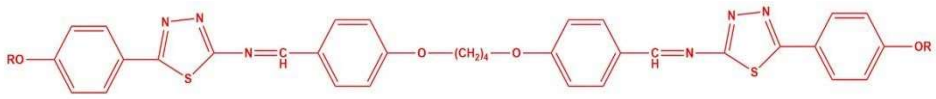

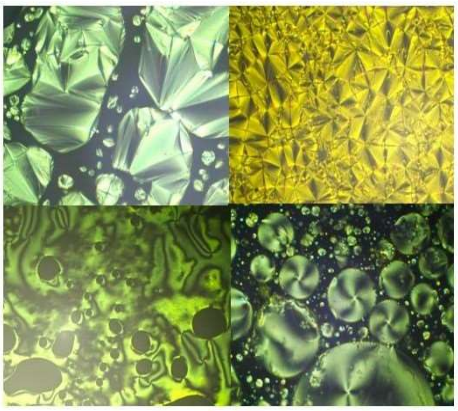

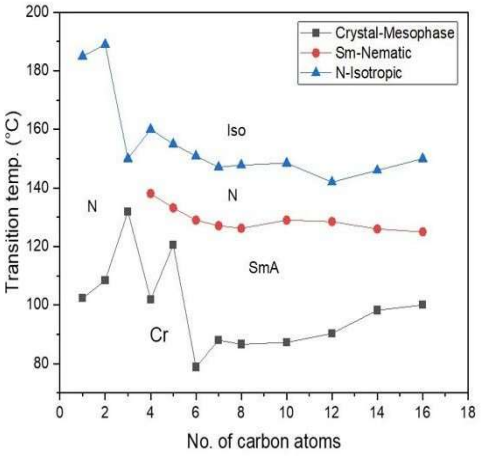

Synthesis, characterization, and mesomorphic behaviour of novel thiadiazole derivatives having azomethine linkages

2.1. Introduction

Numerous mesogenic 1,3,4-thiazoles have been synthesized, according to a review of the liquid crystal literature, even though these materials chemical structures exhibit very little diversity. At the 2nd and 5th positions of the 1,3,4-thiadiazole ring, the substituents such as two aryl-based units, an azo amide or azomethine derivatives, two cycloalkyl units, an alkyl and amino-based units, two cycloalkyl units, an aryl and amino-based derivatives, perfluoroalkyl and an aryl unit derivatives and an aryl and amino unit derivatives have been added. Various mesogenic compounds [1-10] are shown in the Figure 2.1.

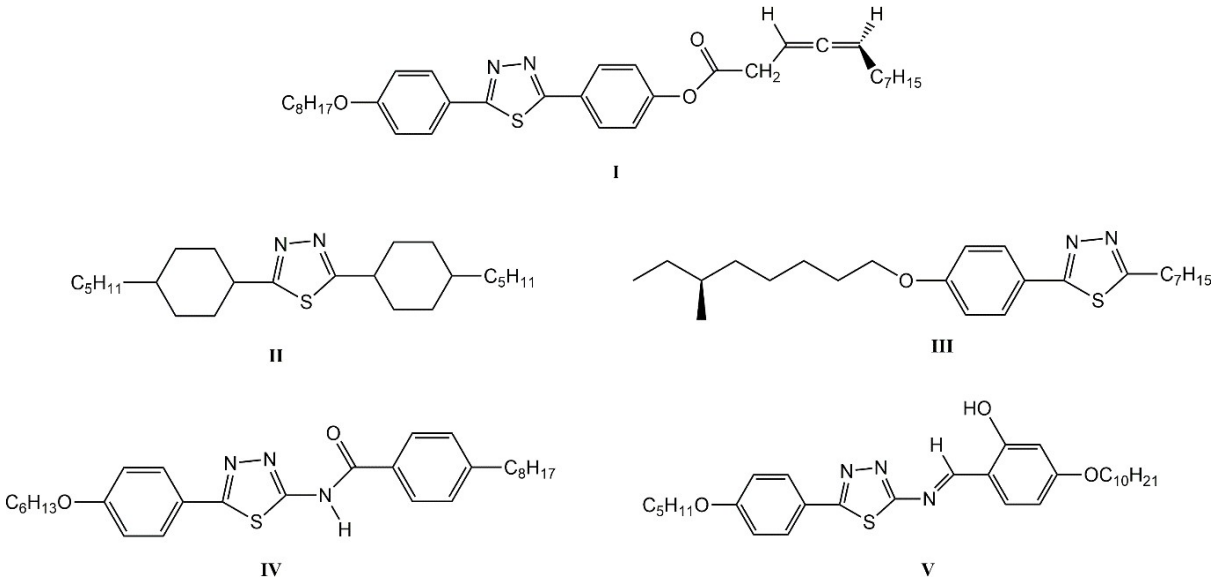

Figure 2.1: Mesogenic 1,3,4-thiadiazole derivatives.

It has been widely known that the thermotropic scheme has existed since Vorlander's research at the turn of the century. The synthesis of the compounds is explained. A large class of lath-shaped molecules with linear mesogenic centers can achieve calamitic mesomorphism [11]. It has proven possible to create mesomorphic compounds using heterocyclic units, and interest in these kinds of structures is always rising. The mesomorphic behaviour of calamitic molecules is significantly influenced by the introduction of heterocycles within their central core. This is partly because of the dipolar moment linked to the heterocyclic ring [12-16]. Liquid crystalline materials have a wide range of applications in the optical [17], electrical [18], and biological fields [19], making their study interesting. It is generally found that the

introduction of a flexible chain into liquid crystalline molecules can lower their melting point, improving the stability of the mesogenic materials. It was found that the conformation of molecules as well as intermolecular interactions can have an impact on the liquid crystalline properties. Many mesomorphic compounds with heterocyclic units have been synthesized in the past few decades [20, 21]. There is a large growing interest in the compounds where the heteroatoms are introduced and due to this, it influences the physical properties and the mesomorphic behavior of the compounds. Thiadiazole [22-26] has also been suggested to be a part of the molecular moiety of calamitic mesogens. New mesogenic units can be formed when a thiadiazole ring is added to the fundamental structure of heteroaromatic systems. The type and phase transition temperatures of the mesophases can be affected by the heteroatoms, which can also significantly alter the polarity, polarizability, and shape of the molecules [27-34].

Organic compounds with a disc shape, such as phthalocyanine, triphenylene, and benzene, may display mesomorphic characteristics when encircled by several aliphatic chains. Nowadays, people refer to these as discotic liquid crystals. Chandrasekhar *et al.* discovered the first examples of these compounds in 1977 [35]. These materials have gained a great deal of attention in materials research during the last fourty years, and as of right now, the literature lists over four thousand different types of discotic liquid crystals. These materials generally exhibit nematic (with only orientational order) or columnar (with both orientational and positional order) mesophases, depending on molecular interactions, orientation, and positional order. The nematic and columnar phases hold significant importance when it comes to the application of devices. To improve the viewing angle of frequently used twisted nematic LCDs, polymerized discotic nematic liquid crystal films have been commercialized as negative birefringence compensation films [35]. It has also been established that they can be used as an active component in wide-viewing LCDs [36, 37]. The gadgets made with discotic nematic liquid crystals based on hexaalkynylbenzene are easy to assemble and have big, symmetrical viewing angle properties. Many liquid crystalline compounds have been synthesized using azomethine linkers. Nematic and/or smectic mesophases are improved by calamitic Schiff base liquid crystals, which resemble rods [38]. The soft materials transition state is significantly influenced by the steric packing factors. Hence, the synthesis of traditional thermotropic liquid crystalline compounds requires anisotropic calamitic or discotic molecular structures as a basic condition. Calamitic materials mesomorphic properties are mostly determined by their molecular structure, where even little changes in molecular structure can have a significant impact on mesomorphic properties. Since the discovery of nematogenic 4-

methoxybenzylidene-4C-butylaniline at room temperature [39], the majority of research has been directed at imine linkages. An effective technique for altering a compound's geometrical structure may increase its thermal stabilities and expand its mesomorphic range [40-42]. As a result, calamitic thermotropic liquid crystals with terminal substituents have received a lot of attention. In general, significant variations in mesomorphic behaviour can be obtained depending on the kind and size of terminal groups [43, 44]. Furthermore, it was discovered that changes in the length or electronic nature of terminal chains affected the structural compound's core rigidity, which in turn affected the compounds linearity to some extent because more chain configurations resulted in varied terminal and parallel interactions. The mesomorphic properties are also significantly influenced by the excluded volume and molecule shape. Moreover, the mesogenic core and the competing parallel and terminal intermolecular interactions are crucial to the mesomorphic behaviour of liquid crystalline materials, and this is typically explained in terms of molecular shape. It has been noted recently that when the length of the terminal substituent increases, the molecular architecture tends to be more parallelly arranged. Furthermore, the terminal chains provide the chiral mesophases as well as the heliconical and twist-bend nematic phases [45, 46]. While many terminals have been generated in the creation of mesomorphic materials, using an alkyl/alkoxy chain or a short compact polar substituent is the most common approach [47].

Although only a small number of structural alterations have been explored, 1,3,4-thiadiazoles are very abundant in the literature. Most systems attribute compounds in place of the 1,3,4-thiadiazole core at the 2nd and 5th position. Appropriate diacylhydrazines are sulfurized and cyclized to form these compounds. A significant lateral dipole is imparted from S to the N-N bond (3.0 D) center by the 1,3,4-thiadiazole core [48].

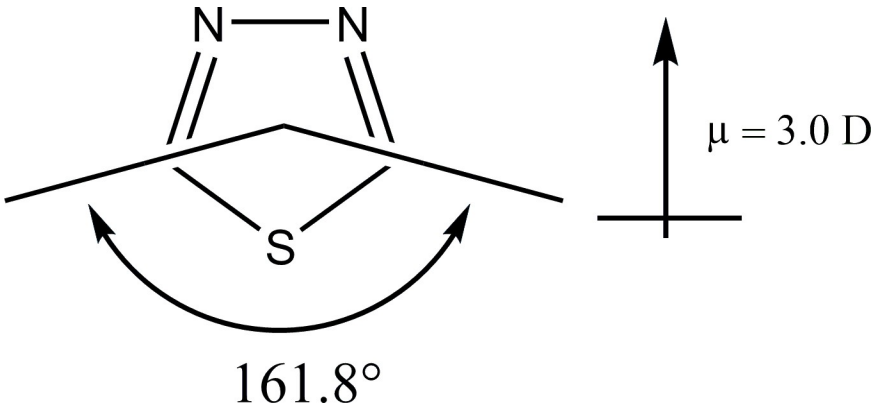

Figure 2.2: Geometry of 1,3,4-thiadiazole

For nonlinear optical (NLO) applications, Tschierske *et al*. reported in 1995 on a new synthesis of different thiadiazoles [49]. Additionally, Tschierske *et al*. have synthesized different mesogens that contain an asymmetric allene group, making them axially chiral. The benefit of using the 1,3,4-thiadiazole moiety is that it provides a donor-acceptor n-system in the proper orientation without changing the molecules rod-like form by adding large lateral substituents. Therefore, adding a chromophore system to enhance the NLO effect does not affect the mesomorphic features. Indeed, the propensity of thiadiazole derivatives to produce smectic mesophase is widely recognized.

Parra *et al.* have studied many thiadiazole compounds including connecting groups consisting of amide [50, 51], imine, and azo derivatives. Additionally, they have discovered the first derivatives of amino-thiadiazole that display columnar liquid crystalline behaviour. This has created a wide opportunity to invent novel thiadiazole derivatives that may display intriguing columnar mesomorphic behaviour. Complexes of azo compounds (including a terminal thiadiazole ring) with n-alkoxybenzoic acids have been studied by Lai *et al.* [52].

Xu *et al.* employed a strategy [53], selecting a suitable thiosemicarbazone as the primary precursor. There have also been reports of 1,3,4-thiadiazole-2-carboxylate esters and ester-linked ferroelectric 1,3,4-thiadiazole [54]. A few novel 1,3,4-thiadiazole compounds that are 2,5-disubstituted exhibit antituberculosis action [55]. Additionally, they might be utilized to create brand-new fused heterocyclic systems that specifically target 2,6-disubstituted imidazoles. Thiadiazole is made using a variety of synthetic techniques [56, 57]. By adding a 2,5-thiadiazole moiety to the crown ether framework through carbon-oxygen bonds created by the reaction of 2,5-dichloro-1,3,4-thiadiazole with polyethene glycols, Pati *et al.* have developed macrocyclic molecules. It has been demonstrated that certain substances have special chemical and biological characteristics [58]. The crystalline and optical characteristics of hyper-branched polymers with an internal 2,5-diphenyl-1,3,4-thiadiazole as a mesogen have been developed by Sato *et al*. [59]. New 5-substituted 1,3,4-thiadiazole-2-carboxylate esters have been produced by Bradley *et al.* [60] through the ring closure of suitable tricarbonyl precursors. By acylating the hydrazones of oxamic acid the hydrazides, Yarovenko *et al*. have created a technique for producing derivatives of 4,5-dihydro-1,3,4-thiadiazole-2-carboxamide. In the synthesis of 3-alkyl/aryl-6-(1-chloro-3,4-dihydronaphth-2-yl)-5,6-dihydro-s-triazolo thiadiazoles under microwave irradiation has been described by Kamotra *et al.* [61, 62].

A ferroelectric 1,3,4-thiadiazole with increased NLO activity and chirality, as well as a chiral thioalkyl substituent at the second position of the thiadiazole ring, was synthesized and published by Loos-Wildenauer *et al*. in 1995. The di-potassium salt of aroyldithiocarbazate was formed by the reaction of 4-hydroxybenzohydrazide **(1)** with carbon disulfide and potassium hydroxide, which initiated the heterocycle's synthesis. 1,3,4-thiadiazolin-2-thione was produced by acidifying freshly made aroyldithiocarbamate at 0 to -5 °C and concurrently cyclizing it. Since thione cannot be directly alkylated, it is the most stable tautomeric form. An effective etherification precursor is produced by the thiadiazole disulfide's formation and the phenolic -OH group's protection.

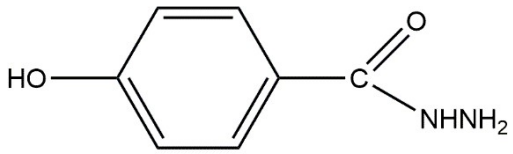

1

Figure 2.3: Chemical structure of 4-hydroxybenzohydrazide (**1**).

A relatively new type of mesogen is liquid crystalline thiadiazoles with a connecting group between the thiadiazole ring and another aryl group.

Parra *et al.* have developed a substantial amount of literature in this field, with their synthesis focusing on 2-amino-1,3,4-thiadiazole building blocks. The thiadiazole's amine moiety has been converted into amide, imine, and azo linking groups. In a mixture of strong hydrochloric acid and ethanol, hydrazide **(2)** was reacted with ammonium thiocyanate to yield thiosemicarbazide, which on further cyclization and concurrent dehydration upon reaction with acetyl chloride gives corresponding thiadiazoles, on further acid hydrolysis yields amino-thiadiazole **(3)**, which was then heated to 140 °C with aromatic aldehydes to yield imines.

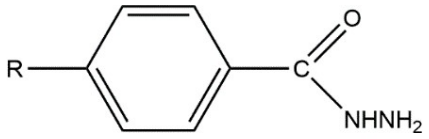

2

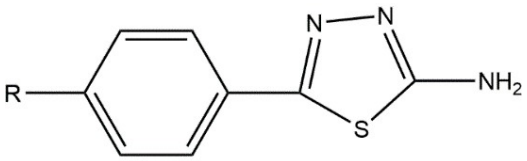

3

Figure 2.4: Chemical structures of hydrazide (**2**) and amino-thiadiazole (**3**).

Under microwave irradiation and solvent-free conditions, Han *et al.* [63] have synthesized a series of 2-(4-alkoxyphenyl)-5-p-tolyl-1,3,4-thiadaizoles in high yields. The same 2,5-diphenyl-1,3,4-thiadiazole unit, linked by an alkoxy chain and a terminal methyl group, is present in all of these compounds. Richer mesophases and broader mesomorphic temperature ranges are frequently seen in mesogenic 1,3,4-thiadiazole compounds with the terminal methyl group compared to their equivalents with other groups [64]. Moreover, it is simple to structurally modify molecules having an end methyl group to form a variety of mesomorphic materials. Across a broad temperature range, all of these compounds display stable liquid crystal behaviour. In addition to being mesogenic, the lower homologue has the shortest alkyl ($-CH_3$) and alkoxy ($-OCH_3$) chains. The structure-property relationship reveals that the bent-shaped molecules cause the mesomorphic properties in all compounds with a central furan ring to vanish, while the linear molecules fascinate to form stable mesophases with wide mesomorphic temperature ranges.

Seltmann and Lehmann have reported several symmetric and non-symmetric V-shaped nematic mesogens with a 1,3,4-thiadiazole bending unit [65]. Comparing the derivatives with unsubstituted terminal alkyl chains, the transition temperatures are considerably lowered by terminal ester groups. The mesophase stability did not increase any further in the case of a mesogen with four different chains. In subsequent instances of molecular engineering, the selection of chain length is likely to play a significant role. The liquid crystalline phases in the enantiotropic interval of the LC phases were found to be uniaxially nematic by investigation

employing POM and DSC. X-ray investigations, however, revealed that these uniaxial phases were made up of tiny biaxial domains.

The impact of monomer configurations on the liquid crystalline and optical characteristics of hyperbranched polymers with an internal 2,5-diphenyl-1,3,4-thiadiazole as a mesogen has been assessed by Sato *et al.* [66]. Among these, thermotropic smectic phases were generated independently of feed mole ratios by polymers including short aliphatic spacers between the core site of monomers and the 2,5-diphenyl-1,3,4-thiadiazole unit. Hyper-branched polymers in solutions exhibited peak maxima at the same wavelength in their UV-vis absorption and PL spectra, regardless of the feed mole ratios of the monomer structures.

We synthesized two symmetrical homologous series of Schiff's-bases derived from the condensation of 1,4-bis(4'-formylphenoxy)butane and 1,3-bis(4'-formylphenoxy)propane with the appropriate 5-(4'-alkoxyphenyl)-1,3,4-thiadiazol-2-amine. The structure of the thiadiazole molecule is the most significant and versatile area of research which motivates us to study the liquid crystal properties. The structure-property relationship was carefully studied. The thermal stability was assessed using thermogravimetry analysis.

2.2. Experimental Section

2.2.1 Materials and Measurements

The synthetic strategy employed to prepare mesomorphic compounds is described in Scheme 2.1. The prepared compounds were elucidated using spectroscopic techniques. All the chemicals and solvents were purchased from a local supplier and used in a reaction without further purification. 4-hydroxybenzaldehyde from Sigma Aldrich, acetone from SD Fine Chem. Limited, 1,3-dibromopropane, 1,4-dibromobutane from Spectrochem Pvt. Limited, potassium carbonate, p-hydroxybenzoic acid, potassium hydroxide, ethanol, hydrochloric acid, thiosemicarbazide, sulphuric acid, glacial acetic acid from Lobachemie Pvt. Limited. Thin Layer Chromatography (Merck 60 F245) was performed on silica gel plates with examination under UV light.

FT-IR spectra were determined for KBr pellets using a Perkin Elmer Spectrum Two. Using deuterated chloroform ($CDCl_3$) as the solvent and an Avance Bruker 400 spectrophotometer (400 MHz) to record the ^1H NMR spectra, TMS was used as the internal standard. To assess the thermal behavior of prepared compounds, a Nikon Eclipse Ci-Pol microscope (Japan) with

a Linkam heating stage, at 10 °C/min heating rate was used. Differential Scanning Calorimetry (DSC-822, Mettler Toledo having Stare software) with platinum pans was also used. To determine the compounds' thermal stability, about 2-3 mg of the sample was placed in a thermogravimetric analyzer (TGA-50, Shimadzu Japan). The elemental analysis was performed using a Thermo Finnigan (Flash 1112 series EA) CHN analyzer.

2.2.2 Synthesis and Characterization

2.2.2.1 Synthesis of bis (4'-formylphenoxy)alkane (1) [67]

A mixture of 4-hydroxybenzaldehyde (0.016 mol), potassium carbonate (0.033 mol) dry acetone (50 mL), and an appropriate amount of 1,3-dibromopropane/1,4-dibromobutane (0.008 mol) was refluxed for 6 h. After filtration, the final product was obtained. The product was cooled and the purification was carried out by recrystallization method (using ethanol as a solvent). The melting point is in good accordance with the literature. Yield: 75%.

2.2.2.2 Synthesis of 4-n-(alkoxy)benzoic acid (2a-2l) [68]

A suitable alkyl halide (0.12 mol), potassium hydroxide (0.1 mol), and p-hydroxybenzoic acid (0.036 mol) were dissolved in ethanol (40 mL) and refluxed for 8–10 h. To hydrolyze the ester formed, after adding 25 mL of a 10% aqueous KOH solution, reflux was carried out for 4-5 h. The obtained solution was chilled and acidified with cold HCl. Until steady transition temperatures were attained, 4-n-alkoxy acids were purified using the recrystallization process. Yield: 80-85%.

2.2.2.3 Synthesis of 5-(4'-alkoxyphenyl)-1,3,4-thiadiazol-2-amine (3a-3l) [69]

An alcoholic solution of 4-n-alkoxybenzoic acid (0.01 mol) was mixed with an aqueous solution of thiosemicarbazide (0.01 mol) with continuous stirring. A drop or two of concentrated sulfuric acid was added to the solution was refluxed for 4 h, The crude product was obtained, filtered out, cleaned with cold water, and recrystallized from appropriate solvent. Yield: 75-80%.

2.2.2.4 Synthesis of Final Compound (4a-4l) and (5a-5l) [Series-I and II]

The condensation reaction between bis(4'-formylphenoxy)alkane (1) and 5-(4'-alkoxyphenyl)-1,3,4-thiadiazol-2-amine (3a-l) results in the final Schiff's base derivatives. In general, 1,4-bis(4'-formylphenoxy)butane (0.001 mol) and 5-(4'-alkoxyphenyl)-1,3,4-thiadiazol-2-amine (0.2 mol) were dissolved in 10 mL of EtOH and a drop or two of glacial AcOH were used as a catalyst. Reflux for 3-4 h. After the completion of the reaction, the liquid was cooled, poured into ice, filtered out, cleaned with cold water, and then recrystallized with ethanol to get the desired result.

1,1'-(butane-1,4-diylbis(oxy))bis(4,1-phenylene))bis(N-5-(4-methoxyphenyl)-1,3,4-thiadiazol-2-yl)methanimine) (4a)

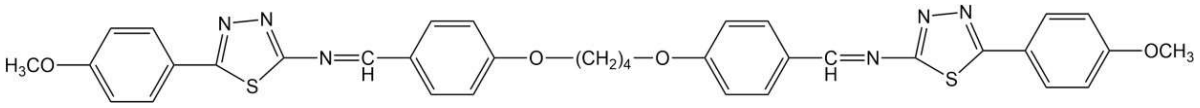

Creamy crystalline solid; **IR** ν_{max} (KBr, cm^{-1}) 2983, 2956, 2843 (ν C-H aliphatic), 1604 (ν C=N), 1578, 1510, 1467, 1450, 1427 (ν C=C aromatic), 1261 (ν Ar-O-R), 1180, 1168, 1157 (ν C-N), 697 (ν C-S-C). **^{1}H NMR** (400 MHz, $CDCl_3$, TMS) δ_H 2.04-2.07(m, 4H, $-CH_2-CH_2-$), 3.90-3.91(s, 6H, $-CH_3$), 4.14-4.17(t, 4H, Ar-OCH_2-), 6.95(d, 2H, J = 9.2 Hz, Ar-H), 6.98(d, 2H, J = 4.8 Hz, Ar-H), 7.03(d, 4H, J = 8.4 Hz, Ar-H), 7.62(d, 2H, J = 8.8 Hz, Ar-H), 7.85(d, 2H, J = 2.4 Hz, Ar-H), 7.87(d, 2H, J = 5.2 Hz, Ar-H), 8.10(d, 2H, J = 2.4 Hz, Ar-H), 8.61, 8.99(s, 2H, -CH=N-). **^{13}C NMR** (100 MHz, $CDCl_3$): δc 25.81, for methylene carbons ($-CH_2-CH_2-$), 55.45, 55.51 ($-CH_3$), 67.76, 68.80 (Ar-OCH_2-), 113.76, 114.73, 114.86, 114.97, 115.21, 115.40, 116.50, 117.90, 118.90, 119.90, 121.57, 121.58, 129.18, 129.50, 129.61, 129.72, 129.80, 129.81, 129.89, 129.90, 129.95, 132.06, 132.36 for aromatic carbons, 163.97, 164.00 (-CH=N-), 170.75, 171.70 (-C=N- thiadiazole).

i1,1'-(butane-1,4-diylbis(oxy))bis(4,1-phenylene))bis(N-5-(4-ethoxyphenyl)-1,3,4- thiadiazol-2-yl)methanimine) (4b)

1,1'-(butane-1,4-diylbis(oxy))bis(4,1-phenylene))bis(N-5-(4-ethoxyphenyl)-1,3,4-thiadiazol-2-yl)methanimine) (4b)

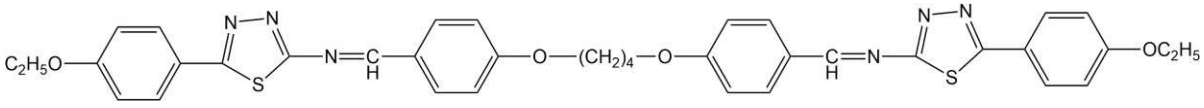

White crystalline solid; **IR** ν_{max} (KBr, cm^{-1}) 2986, 2945, 2890, 2838 (ν C-H aliphatic), 1607 (ν C=N), 1578, 1510, 1468, 1431 (ν C=C aromatic), 1263 (ν Ar-O-R), 1175, 1157, 1124 (C-N), 697 (ν C-S-C). **^{1}H NMR** (400 MHz, $CDCl_3$, TMS) δ_H 1.45-1.47(t, 6H, $-CH_3$), 1.48-1.49(m, 4H, $-CH_2-CH_2-$), 4.10-4.14(t, 4H, Ar-OCH_2-), 4.15-4.17(d, 4H, Ar-O-CH_2-), 6.96(d, 4H, J = 8.8

Hz, Ar-H), 7.03(d, 4H, *J* = 8.8 Hz, Ar-H), 7.85(d, 2H, *J* = 2.8 Hz, Ar-H), 7.86(d, 2H, *J* = 5.2 Hz, Ar-H), 8.06(d, 2H, *J* = 1.6 Hz, Ar-H), 8.08(d, 2H, *J* = 2 Hz, Ar-H), 8.70, 8.99(s, 2H, -CH=N-). **^{13}C NMR** (100 MHz, $CDCl_3$)): δ 14.48, 14.68 ($-CH_3$), 25.81, 27.81, for methylene carbons ($-CH_2-CH_2-$), 63.78, 67.76, 67.80, 67.90 ($Ar-OCH_2-$), 114.18, 114.73, 114.80, 114.90, 121.35, 121.40, 121.60, 129.80, 129.81, 129.85, 129.90, 129.91, 129.92, 129.96, 132.05, 132.34 for aromatic carbons, 163.43, 163.97 (-CH=N-), 170.84, 170.90 (-C=N- thiadiazole).

1,1'-(butane-1,4-diylbis(oxy))bis(4,1-phenylene))bis(N-5-(4-propoxyphenyl)-1,3,4-thiadiazol-2-yl)methanimine) (4c)

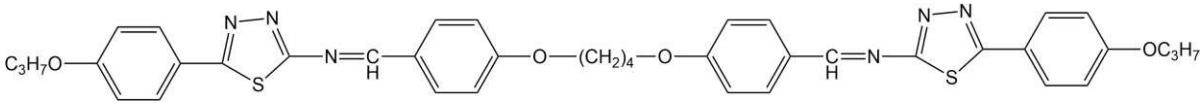

Pale yellow crystalline solid; **IR** ν_{max} (KBr, cm^{-1}) 2969, 2948, 2882, 2795 (*v* C-H aliphatic), 1607 (*v* C=N), 1595, 1577, 1512, 1478, 1466, 1446, 1423, 1410 (*v* C=C aromatic), 1251 (*v* Ar-O-R), 1164, 1130, 1115 (*v* C-N), 693 (*v* C-S-C). **^{1}H NMR** (400 MH_Z, $CDCl_3$, TMS) δ_H 1.05-1.07(t, 6H, $-CH_3$), 1.83-1.85(m, 4H, $-C\underline{H}_2-CH_3$), 1.87-1.89(m, 4H, $-CH_2-CH_2-$), 4.01-4.03(t, 4H, $Ar-OCH_2-$), 4.14-4.17(t, 4H, $Ar-O-CH_2-$), 6.95(d, 2H, *J* = 2 Hz, Ar-H), 6.97(d, 2H, *J* = 2 Hz, Ar-H), 7.01(d, 2H, *J* = 2.4 Hz, Ar-H), 7.03(d, 2H, *J* = 2 Hz, Ar-H), 7.85(d, 2H, *J* = 2.8 Hz, Ar-H), 7.86(d, 2H, *J* = 4.8 Hz, Ar-H), 8.09(d, 2H, *J* = 2.8 Hz, Ar-H), 8.06(d, 2H, *J* = 2.8 Hz, Ar-H), 8.60, 8.98(s, 2H, -CH=N-). **^{13}C NMR** (100 MHz, $CDCl_3$): δc 10.48, 10.49 ($-CH_3$), 22.45, 22.50, 25.81, 25.90, for methylene carbons ($-CH_2-CH_2-$), 67.76, 67.80, 67.90, 69.75 ($Ar-OCH_2-$), 114.20, 114.40, 114.70, 114.73, 114.80, 121.33, 122.23, 129.70, 129.80, 129.95, 132.05, 132.06, 132.34 for aromatic carbons, 163.67, 163.97 (-CH=N-), 171.39, 171.90 (-C=N- thiadiazole).

1,1'-(butane-1,4-diylbis(oxy))bis(4,1-phenylene))bis(N-5-(4-butoxyphenyl)-1,3,4-thiadiazol-2-yl)methanimine) (4d)

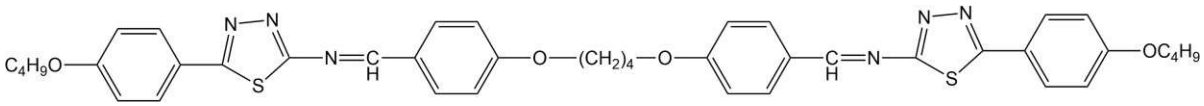

Pale yellow crystalline solid**; IR** ν_{max} (KBr, cm^{-1}) 2955, 2931, 2873 (*v* C-H aliphatic), 1606 (*v* C=N), 1578, 1511, 1467, 1449, 1426 (*v* C=C aromatic), 1255 (*v* Ar-O-R), 1173, 1157, 1124, 1110 (*v* C-N), 697 (*v* C-S-C). **^{1}H NMR** (400 MH_Z, $CDCl_3$, TMS) δ_H 0.99-1.02(t, 6H, $-CH_3$), 1.50-1.78(m, 8H, $-CH_2-CH_2-$), 1.80-1.83(m, 4H, $-CH_2-CH_2-$), 4.04-4.07(t, 4H, $Ar-OCH_2-$),

4.14-4.17(t, 4H, Ar-O-CH_2-), 6.94(d, 2H, *J* = 2 Hz, Ar-H), 6.96(d, 2H, *J* = 4.8 Hz, Ar-H), 7.01(d, 2H, *J* = 2 Hz, Ar-H), 7.02(d, 2H, *J* = 5.2 Hz, Ar-H), 7.85(d, 2H, *J* = 2 Hz Ar-H), 7.87(d, 2H, *J* = 1.6 Hz, Ar-H), 8.06(d, 2H, *J* = 2 Hz, Ar-H), 8.07(d, 2H, *J* = 5.2 Hz, Ar-H), 8.58, 8.97(s, 2H, -CH=N-). **^{13}C NMR** (100 MHz, $CDCl_3$) δc 13.83, 14.81 (-CH_3), 19.10, 19.20 (-$\underline{C}H_2$-CH_3), 25.81, 25.90, 31.10, 31.13, for methylene carbons (-CH_2-CH_2-), 67.78, 67.80, 68.90, 69.85 (Ar-OCH_2-), 114.20, 114.30, 114.40, 114.60, 114.73, 121.32, 121.60, 122.21, 122.22, 122.50, 122.60, 129.98, 130.10, 132.06, 132.33 for aromatic carbons, 163.67, 163.97 (-CH=N-), 171.25, 171.30 (-C=N- thiadiazole).

1,1'-(butane-1,4-diylbis(oxy))bis(4,1-phenylene))bis(N-5-(4-pentyloxyphenyl)-1,3,4-thiadiazol-2-yl)methanimine) (4e)

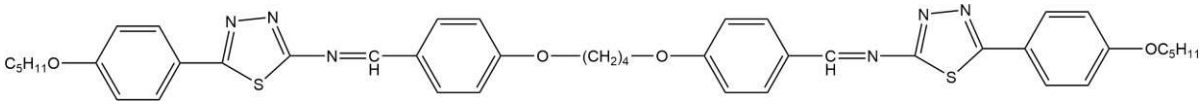

Light yellow crystalline solid**; IR** ν_{max} (KBr, cm^{-1}) 2953, 2935, 2871, 2857 (*ν* C-H aliphatic), 1605 (*ν* C=N), 1577, 1511, 1468, 1429 (*ν* C=C aromatic), 1260 (*ν* Ar-O-R), 1168 (*ν* C-N), 697 (*ν* C-S-C). **^{1}H NMR** (400 MHz, $CDCl_3$, TMS) δ_H 0.96-0.98(t, 6H, -CH_3), 1.40-1.42(m, 4H, -CH_2-CH_2-), 1.42-1.44(m, 4H, -$\underline{C}H_2$-CH_3), 1.81(m, 2H, -CH_2-CH_2-), 1.82(m, 2H, -CH_2-CH_2-), 1.83-1.85(m, 4H, -CH_2-CH_2-), 4.03-4.04(t, 4H, Ar-OCH_2-), 4.06-4.16(t, 4H, Ar-O-CH_2-), 6.94(d, 2H, *J* = 2 Hz, Ar-H), 6.96(d, 2H, *J* = 2 Hz, Ar-H), 7.01(d, 2H, *J* = 1.6 Hz, Ar-H), 7.02(d, 2H, *J* = 5.2 Hz, Ar-H), 7.85(d, 2H, *J* = 2 Hz, Ar-H), 7.87(d, 2H, *J* = 1.6 Hz, Ar-H), 8.06(d, 2H, *J* = 2 Hz, Ar-H), 8.07(d, 2H, *J* = 4.8 Hz, Ar-H), 8.61, 8.91(s, 2H, -CH=N-). **^{13}C NMR** (100 MHz, $CDCl_3$) δc 14.01, 14.10 (-CH_3), 22.45, 22.48 (-$\underline{C}H_2$-CH_3), 28.14, 28.16, 28.80, 28.90, for methylene carbons (-CH_2-CH_2-), 67.76, 67.80, 68.28, 68.30 (Ar-OCH_2-), 114.20, 114.30, 114.42, 114.62, 114.73, 121.32, 121.65, 122.21, 122.22, 122.50, 122.60, 129.80, 129.98, 130.10, 132.07, 132.34 for aromatic carbons, 163.67, 163.68 (-CH=N-), 171.38, 171.39 (-C=N-thiadiazole).

1,1'-(butane-1,4-diylbis(oxy))bis(4,1-phenylene))bis(N-5-(4-hexyloxyphenyl)-1,3,4-thiadiazol-2-yl)methanimine) (4f)

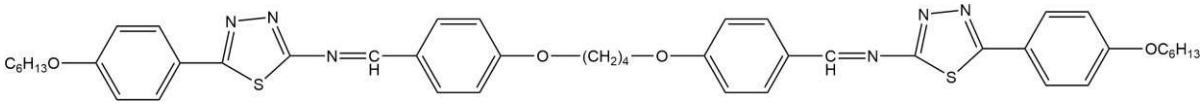

White crystalline solid; **IR** ν_{max} (KBr, cm^{-1}) 2953, 2935, 2870, 2854, 2791, 2718 (ν C-H aliphatic), 1607 (ν C=N), 1580, 1512, 1447, 1446, 1428 (ν C=C aromatic), 1258 (ν Ar-O-R), 1607 (ν C-N), 695 (ν C-S-C). **^{1}H NMR** (400 MHz, $CDCl_3$, TMS) δ_H 0.90-0.91(t, 6H, $-CH_3$), 1.39-1.42(m, 8H, $-CH_2-CH_2-$), 1.43-1.45(m, 4H, $-\underline{C}H_2-CH_3$), 1.80-1.81(m, 4H, $-CH_2-CH_2-$), 1.88-1.89(m, 4H, $-CH_2-CH_2-$), 4.04-4.05(t, 4H, Ar-O-CH_2-), 4.10-4.12(t, 4H, Ar-O-CH_2-), 7.01(d, 2H, J = 1.8 Hz, Ar-H), 7.02(d, 2H, J = 4 Hz, Ar-H), 7.05(d, 2H, J = 4 Hz, Ar-H), 7.08(d, 2H, J = 4 Hz, Ar-H), 7.85(d, 2H, J = 2 Hz, Ar-H), 7.87(d, 2H, J = 1.4 Hz Ar-H), 8.02(d, 2H, J = 4 Hz, Ar-H), 8.04(d, 2H, J = 4.4 Hz, Ar-H), 8.68, 8.81(s, 2H, -CH=N-). **^{13}C NMR** (100 MHz, $CDCl_3$) δc 14.04, 14.06 ($-CH_3$), 22.60, 22.68 ($-\underline{C}H_2-CH_3$), 25.10, 25.15, 28.90, 28.91, 29.14, 29.16, 31.10, 31.18 for methylene carbons ($-CH_2-CH_2-$), 67.78, 67.88, 68.30, 68.32 (Ar-OCH_2-), 114.22, 114.32, 114.42, 114.62, 114.72, 114.30, 114.31, 121.30, 121.35, 121.60, 121.65, 122.21, 122.24, 122.50, 122.60, 129.80, 129.98, 130.10, 132.07, 132.34 for aromatic carbons, 163.70, 163.72 (-CH=N-), 171.40, 171.44 (-C=N- thiadiazole).

1,1'-(butane-1,4-diylbis(oxy))bis(4,1-phenylene))bis(N-5-(4-heptyloxyphenyl)-1,3,4-thiadiazol-2-yl)methanimine) (4g)

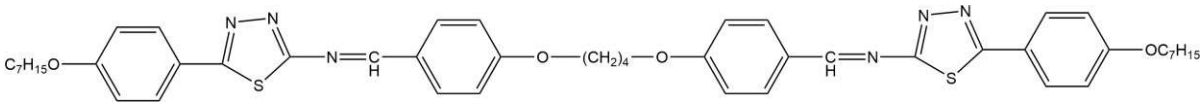

Off-white crystalline solid; **IR** ν_{max} (KBr, cm^{-1}) 2952, 2935, 2852, 2793 (ν C-H aliphatic), 1607 (ν C=N), 1579, 1512, 1466, 1428 (ν C=C aromatic), 1257 (ν Ar-O-R), 1173, 1164 (ν C-N), 695 (ν C-S-C). **^{1}H NMR** (400 MHz, $CDCl_3$, TMS) δ_H 0.90-0.91(t, 6H, $-CH_3$), 1.31-1.39(m, 16H, $-CH_2-CH_2-$), 1.80-1.82(m, 4H, $-CH_2-CH_2-$), 1.83-1.84(m, 4H, $-CH_2-CH_2-$), 4.04-4.06(t, 4H, Ar-O-CH_2-), 4.14-4.16(t, 4H, Ar-O-CH_2-), 6.94(d, 2H, J = 2 Hz, Ar-H), 6.95(d, 2H, J = 4.8 Hz, Ar-H), 7.01(d, 2H, J = 1.6 Hz, Ar-H), 7.02(d, 2H, J = 5.2 Hz, Ar-H), 7.85(d, 2H, J = 2 Hz, Ar-H), 7.86(d, 2H, J = 5.2 Hz, Ar-H), 8.06(d, 2H, J = 2 Hz, Ar-H), 8.08(d, 2H, J = 5.2 Hz, Ar-H), 8.55, 8.91(s, 2H, -CH=N-). **^{13}C NMR** (100 MHz, $CDCl_3$): δc 14.10, 14.18 ($-CH_3$), 22.61, 22.62 ($-\underline{C}H_2-CH_3$), 25.81, 25.85, 25.95, 25.96, 29.04, 29.06, 29.10, 29.20, 31.77, 31.81 for methylene carbons ($-CH_2-CH_2-$), 67.76, 67.78, 68.30, 68.32 (Ar-OCH_2-), 114.20, 114.22, 114.32, 114.52, 114.72, 114.73, 114.30, 114.31, 121.36, 121.38, 121.40, 121.60, 122.21, 122.24, 122.40, 122.62, 129.82, 129.90, 132.06, 132.10, 132.34 for aromatic carbons, 163.68, 163.97 (-CH=N-), 171.36, 171.38 (-C=N- thiadiazole).

1,1'-(butane-1,4-diylbis(oxy))bis(4,1-phenylene))bis(N-5-(4-octyloxyphenyl)-1,3,4-thiadiazol-2-yl)methanimine) (4h)

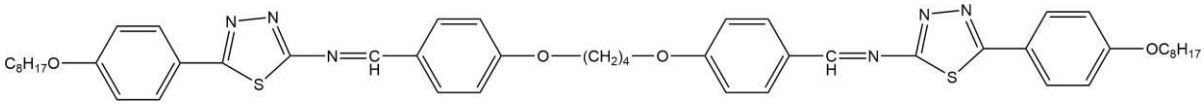

Off-white crystalline solid; **IR** ν_{max} (KBr, cm^{-1}) 2953, 2923, 2850 (ν C-H aliphatic), 1607 (ν C=N), 1578, 1512, 1466, 1428 (ν C=C aromatic), 1257 (ν Ar-O-R), 1165 (ν C-N), 693 (ν C-S-C). **^{1}H NMR** (400 MH_Z, $CDCl_3$, TMS) δ_H 0.89-0.92(t, 6H, $-CH_3$), 1.28-1.39(m, 20H, $-CH_2-CH_2-$), 1.79-1.81(m, 4H, $-CH_2-CH_2-$), 1.83-1.84(m, 4H, $-CH_2-CH_2-$), 4.02-4.06(t, 4H, Ar-O-CH_2-), 4.14-4.17(t, 4H, Ar-O-CH_2-), 6.94(d, 2H, J = 2 Hz, Ar-H), 6.95(d, 2H, J = 4.8 Hz, Ar-H) 7.01(d, 2H, J = 1.6 Hz, Ar-H), 7.02(d, 2H, J = 5.2 Hz, Ar-H), 7.85(d, 2H, J = 2 Hz, Ar-H), 7.86(d, 2H, J = 4.8 Hz, Ar-H), 8.06(d, 2H, J = 2 Hz, Ar-H), 8.08(d, 2H, J = 5.2 Hz, Ar-H), 8.71, 8.91(s, 2H, -CH=N-). **^{13}C NMR** (100 MHz, $CDCl_3$): δc 14.12, 14.14 ($-CH_3$), 22.67, 22.68 ($-\underline{C}H_2-CH_3$), 25.81, 25.99, 29.10, 29.20, 29.23, 29.30, 29.33, 29.38, 31.81, 31.84 for methylene carbons ($-CH_2-CH_2-$), 67.74, 67.5, 67.76, 68.31 (Ar-OCH_2-), 114.20, 114.24, 114.28, 114.30, 114.34, 114.38, 114.40, 114.41, 114.73, 121.36, 121.39, 121.42, 121.65, 122.41, 122.42, 122.44 , 122.60, 129.82, 129.95, 132.07, 132.34 for aromatic carbons, 163.69, 163.98 (-CH=N-), 171.69, 171.70 (-C=N- thiadiazole).

1,1'-(butane-1,4-diylbis(oxy))bis(4,1-phenylene))bis(N-5-(4-decyloxyphenyl)-1,3,4-thiadiazol-2-yl)methanimine) (4i)

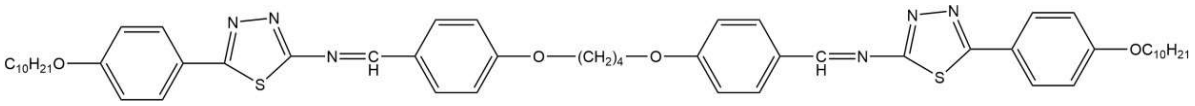

Yellow crystalline solid**; IR** ν_{max} (KBr, cm^{-1}) 2920, 2871, 2852 (ν C-H aliphatic), 1606 (ν C=N), 1578, 1511, 1469, 1428 (ν C=C aromatic), 1256 (ν Ar-O-R), 1170 (ν C-N), 695 (ν C-S-C). **^{1}H NMR** (400 MH_Z, $CDCl_3$, TMS) δ_H 0.88-0.92(t, 6H, $-CH_3$), 1.25-1.36(m, 24H, $-CH_2-CH_2-$), 1.46-1.80(m, 8H, $-CH_2-CH_2-$), 1.82-1.84(m, 4H, $-CH_2-CH_2-$), 4.02-4.05(t, 4H, Ar-O-CH_2-), 4.23-4.28(t, 4H, Ar-O-CH_2-), 7.03(d, 2H, J = 8.8 Hz, Ar-H), 7.05(d, 2H, J = 5.2 Hz, Ar-H), 7.85(d, 2H, J = 2.4 Hz, Ar-H), 7.86(d, 2H, J = 5.2 Hz, Ar-H), 7.87(d, 2H, J = 1.6 Hz, Ar-H), 7.88(d, 2H, J = 2.8 Hz, Ar-H), 8.05(d, 2H, J = 1.6 Hz, Ar-H), 8.06(d, 2H, J = 5.2 Hz, Ar-H), 8.68, 8.90(s, 2H, -CH=N-). **^{13}C NMR** (100 MHz, $CDCl_3$): δc 14.13, 14.14 ($-CH_3$), 22.69, 22.70 ($-\underline{C}H_2-CH_3$), 25.81, 25.84, 25.98, 25.99, 29.09, 29.10, 29.23, 29.30, 29.33, 29.36, 29.40, 29.46, 29.56, 31.90 for methylene carbons ($-CH_2-CH_2-$), 67.76, 67.78, 67.30, 68.32 (Ar-OCH_2-),

114.20, 114.22, 114.30, 114.38, 114.42, 114.44, 114.73, 121.30, 121.36, 121.38, 121.70, 122.45 , 122.48, 122.49, 129.96, 132.06, 132.33 for aromatic carbons, 163.67, 163.97 (-CH=N-), 171.24, 171.30 (-C=N- thiadiazole).

1,1'-(butane-1,4-diylbis(oxy))bis(4,1-phenylene))bis(N-5-(4-dodecyloxyphenyl)-1,3,4-thiadiazol-2-yl)methanimine) (4j)

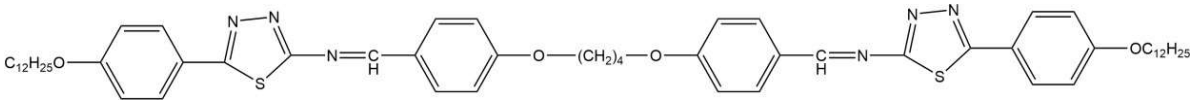

Pale Yellow Crystalline solid; **IR** ν_{max} (KBr, cm^{-1}) 2918, 2850 (ν C-H aliphatic), 1606 (ν C=N), 1578, 1512, 1469, 1427 (ν C=C aromatic), 1257 (ν Ar-O-R), 1171 (ν C-N), 695 (ν C-S-C). **^{1}H NMR** (400 MH_Z, $CDCl_3$, TMS) δ_H 0.88-0.92(t, 6H, $-CH_3$), 1.28-1.37(m, 20H, $-CH_2-CH_2-$), 1.39-1.80(m, 20H, $-CH_2-CH_2-$), 1.82-1.84(m, 4H, $-CH_2-CH_2-$), 4.02-4.06(t, 4H, Ar-O-CH_2-), 4.14-4.17(t, 4H, Ar-O-CH_2-), 6.94(d, 2H, J = 2.4 Hz, Ar-H), 6.95(d, 2H, J = 4.8 Hz, Ar-H), 7.01(d, 2H, J = 1.6 Hz, Ar-H), 7.02(d, 2H, J = 5.2 Hz, Ar-H), 7.85(d, 2H, J = 4.8 Hz, Ar-H), 7.86(d, 2H, J = 4.8 Hz, Ar-H), 8.06(d, 4H, J = 2 Hz, Ar-H), 8.07(d, 2H, J = 4.8 Hz, Ar-H), 8.66, 8.90(s, 2H, -CH=N-). **^{13}C NMR** (100 MHz, $CDCl_3$): δc 14.14, 14.16 ($-CH_3$), 22.71, 22.72 ($-\underline{C}H_2-CH_3$), 25.81, 25.82, 25.98, 25.99, 29.09, 29.11, 29.36, 29.38, 29.57, 29.58, 29.60, 29.62, 29.65, 29.66, 29.67, 29.68, 30.96, 30.98, 31.93, 31.96 for methylene carbons ($-CH_2-CH_2-$), 67.76, 67.79, 68.30, 68.34 (Ar-OCH_2-), 114.20, 114.22, 114.30, 114.32, 114.36, 114.38, 114.40, 114.42, 114.44, 114.46, 114.70, 114.73, 121.32, 121.34, 121.36, 121.38, 122.42, 122.46 , 122.48, 129.96, 132.05, 132.33 for aromatic carbons, 163.67, 163.97 (-CH=N-), 170.40, 171.01 (-C=N- thiadiazole).

1,1'-(butane-1,4-diylbis(oxy))bis(4,1-phenylene))bis(N-5-(4-tetradecyloxyphenyl)-1,3,4-thiadiazol-2-yl)methanimine) (4k)

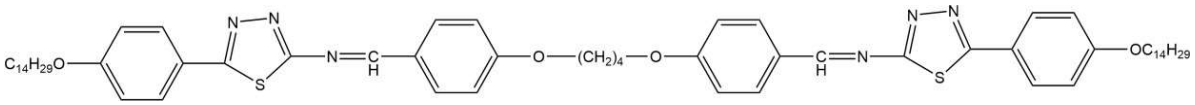

Pale yellow crystalline solid; **IR** ν_{max} (KBr, cm^{-1}) 2920, 2855 (ν C-H aliphatic), 1610 (ν C=N), 1580, 1515, 1470, 1429 (ν C=C aromatic), 1256 (ν Ar-O-R), 1175 (ν C-N), 697 (ν C-S-C). **^{1}H NMR** (400 MH_Z, $CDCl_3$, TMS) δ_H 0.90-0.92(t, 6H, $-CH_3$), 1.26-1.35(m, 24H, $-CH_2-CH_2-$), 1.36-1.39(m, 24H, $-CH_2-CH_2-$), 1.87-1.89(m, 4H, $-CH_2-CH_2-$), 4.01-4.04(t, 4H, Ar-O-CH_2-), 4.20-4.24(t, 4H, Ar-O-CH_2-), 7.01(d, 2H, J = 2.4 Hz, Ar-H), 7.02(d, 2H, J = 4.8 Hz, Ar-H), 7.03(d, 2H, J = 1.6 Hz, Ar-H), 7.05(d, 2H, J = 5.2 Hz, Ar-H), 7.84(d, 2H, J = 4.8 Hz, Ar-H),

7.85(d, 2H, *J* = 4.8 Hz, Ar-H), 8.05(d, 2H, *J* = 2 Hz, Ar-H), 8.06(d, 2H, *J* = 5.2 Hz, Ar-H), 8.60, 8.99(s, 2H, -CH=N-). **^{13}C NMR** (100 MHz, $CDCl_3$): δc 14.15, 14.17 (-CH_3), 22.71, 22.73 (-$\underline{C}H_2$-CH_3), 25.99, 28.97, 28.99, 29.10, 29.20, 29.38, 29.40, 29.57, 29.60, 29.62, 29.67, 29.69, 29.70, 29.71, 29.72, 31.94 for methylene carbons (-CH_2-CH_2-), 63.53, 64.52, 68.20, 67.79, 68.30 (Ar-OCH_2-), 114.20, 114.22, 114.30, 114.33, 114.35, 114.39, 114.42, 114.42, 114.44, 114.46, 114.70, 114.72, 121.32, 121.33, 121.38, 121.39, 122.44, 122.46, 122.48, 129.96, 130.09, 132.06, 132.33 for aromatic carbons, 163.67, 163.77 (-CH=N-), 171.15, 171.18 (-C=N- thiadiazole).

1,1'-(butane-1,4-diylbis(oxy))bis(4,1-phenylene))bis(N-5-(4-hexadecyloxyphenyl)-1,3,4-thiadiazol-2-yl)methanimine) (4l)

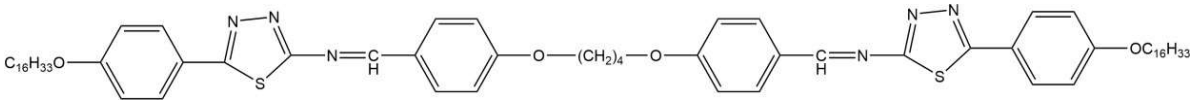

Pale yellow crystalline solid; **IR** ν_{max} (KBr, cm^{-1}) 2930, 2822 (*ν* C-H aliphatic), 1605 (*ν* C=N), 1575, 1520, 1478, 1430 (*ν* C=C aromatic), 1251 (*ν* Ar-O-R), 1180 (*ν* C-N), 696 (*ν* C-S-C). **^{1}H NMR** (400 MH_Z, $CDCl_3$, TMS) δ_H 0.90-0.92(t, 6H, -CH_3), 1.25-1.38(m, 28H, -CH_2-CH_2-), 1.38-1.49(m, 28H, -CH_2-CH_2-), 1.88-1.89(m, 4H, -CH_2-CH_2-), 4.02-4.06(t, 4H, Ar-O-CH_2-), 4.07-4.20(t, 4H, Ar-O-CH_2-), 7.01(d, 2H, *J* = 2 Hz, Ar-H), 7.02(d, 2H, *J* = 4.2 Hz, Ar-H), 7.03(d, 2H, *J* = 1.6 Hz, Ar-H), 7.04(d, 2H, *J* = 5.2 Hz, Ar-H), 7.84(d, 2H, *J* = 4.2 Hz, Ar-H), 7.86(d, 2H, *J* = 4.8 Hz, Ar-H), 8.04(d, 2H, *J* = 2 Hz, Ar-H), 8.06(d, 2H, *J* = 5.2 Hz, Ar-H), 8.58, 8.91(s, 2H, -CH=N-). **^{13}C NMR** (100 MHz, $CDCl_3$: δc 14.13, 14.14 (-CH_3), 22.70, 22.71 (-$\underline{C}H_2$-CH_3), 25.81, 25.82, 25.98, 25.98, 29.10, 29.12, 29.36, 29.38, 29.57, 29.58, 29.60, 29.62, 29.65, 29.66, 29.67, 29.68, 30.96, 30.98, 31.93, 31.96 for methylene carbons (-CH_2-CH_2-), 67.76, 67.79, 68.30, 68.34 (Ar-OCH_2-), 114.20, 114.22, 114.30, 114.32, 114.36, 114.38, 114.40, 114.42, 114.44, 114.46, 114.70, 114.73, 121.32, 121.34, 121.36, 121.38, 122.42, 122.46, 122.48, 129.96, 132.05, 132.33 for aromatic carbons, 163.67, 163.97 (-CH=N-), 170.40, 171.01 (-C=N- thiadiazole).

1,1'-((propane-1,3-diylbis(oxy))bis(4,1-phenylene))bis(N-(5-(4-methoxyphenyl)-1,3,4-thiadiazol-2-yl)methanimine) (5a)

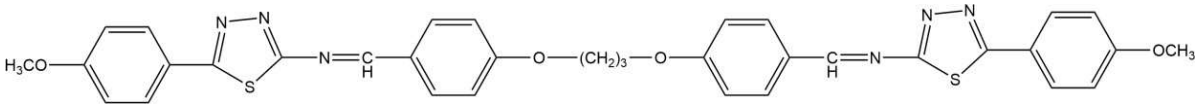

Pale yellow crystalline solid; **IR** ν_{max} (KBr, cm^{-1}) 2985, 2951, 2845 (ν C-H aliphatic), 1606 (ν C=N), 1575, 1515, 1465, 1445, 1430 (ν C=C aromatic), 1262 (ν Ar-O-R), 1178, 1169, 1159 (ν C-N), 697 (ν C-S-C). **^{1}H NMR** (400 MHz, $CDCl_3$, TMS) δ_H 2.01-2.05(m, 2H, -CH_2-CH_2-), 3.89-3.91(s, 6H, -CH_3), 4.10-4.17(t, 4H, Ar-OCH_2-), 6.93(d, 2H, J = 9.2 Hz, Ar-H), 6.96(d, 2H, J = 4.8 Hz, Ar-H), 7.01(d, 4H, J = 8.4 Hz, Ar-H), 7.60(d, 2H, J = 8.8 Hz, Ar-H), 7.84(d, 2H, J = 2.4 Hz, Ar-H), 7.88(d, 2H, J = 5.2 Hz, Ar-H), 8.09(d, 2H, J = 2.4 Hz, Ar-H), 8.58, 8.91(s, 2H, -CH=N-). **^{13}C NMR** (100 MHz, $CDCl_3$): δc 25.81, for methylene carbons (-CH_2-CH_2-), 55.48, 55.52 (-CH_3), 67.75, 68.82 (Ar-OCH_2-), 113.75, 114.74, 114.81, 114.98, 115.23, 115.39, 116.49, 117.67, 118.78, 119.89, 121.50, 121.55, 129.67, 129.68, 129.69, 129.72, 129.80, 129.81, 129.89, 129.90, 129.95, 132.10, 132.36 for aromatic carbons, 163.98, 164.01 (-CH=N-), 170.78, 171.78 (-C=N- thiadiazole).

1,1'-((propane-1,3-diylbis(oxy))bis(4,1-phenylene))bis(N-(5-(4-ethoxyphenyl)-1,3,4-thiadiazol-2-yl)methanimine) (5b)

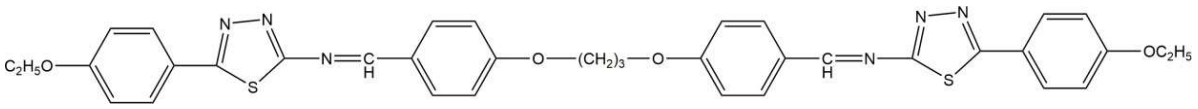

Light yellow crystalline solid; **IR** ν_{max} (KBr, cm^{-1}) 2989, 2942, 2893, 2840 (ν C-H aliphatic), 1609 (ν C=N), 1574, 1509, 1469, 1430 (ν C=C aromatic), 1261 (ν Ar-O-R), 1173, 1159, 1123 (C-N), 696 (ν C-S-C). **^{1}H NMR** (400 MHz, $CDCl_3$, TMS) δ_H 1.44-1.48(t, 6H, -CH_3), 1.46-1.48(m, 2H, -CH_2-CH_2-), 4.09-4.12(t, 4H, Ar-OCH_2-), 4.11-4.14(d, 4H, Ar-O-CH_2-), 6.94(d, 4H, J = 8.8 Hz, Ar-H), 7.01(d, 4H, J = 8.8 Hz, Ar-H), 7.84(d, 2H, J = 2.8 Hz, Ar-H), 7.88(d, 2H, J = 5.2 Hz, Ar-H), 8.05(d, 2H, J = 1.6 Hz, Ar-H), 8.07(d, 2H, J = 2 Hz, Ar-H), 8.69, 8.91(s, 2H, -CH=N-). **^{13}C NMR** (100 MHz, $CDCl_3$)): δ 14.49, 14.70 (-CH_3), 25.80, 27.85, for methylene carbons (-CH_2-CH_2-), 63.78, 67.71, 67.85, 67.93 (Ar-OCH_2-), 114.16, 114.71, 114.84, 114.92, 121.31, 121.43, 121.65, 129.88, 129.90, 129.91, 129.90, 129.91, 129.92, 129.96, 132.05, 132.34 for aromatic carbons, 163.44, 163.96 (-CH=N-), 170.82, 170.91 (-C=N- thiadiazole).

1,1'-((propane-1,3-diylbis(oxy))bis(4,1-phenylene))bis(N-(5-(4-propoxyphenyl)-1,3,4-thiadiazol-2-yl)methanimine) (5c)

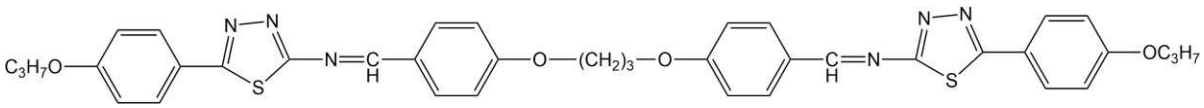

Creamy crystalline solid; **IR** ν_{max} (KBr, cm^{-1}) 2967, 2949, 2881, 2796 (ν C-H aliphatic), 1605 (ν C=N), 1596, 1574, 1509, 1479, 1465, 1449, 1421, 1409 (ν C=C aromatic), 1250 (ν Ar-O-R), 1162, 1129, 1114 (ν C-N), 695 (ν C-S-C). **^{1}H NMR** (400 MHz, $CDCl_3$, TMS) δ_H 1.03-1.05(t, 6H, $-CH_3$), 1.81-1.84(m, 4H, $-CH_2-CH_3$), 1.85-1.87(m, 2H, $-CH_2-CH_2-$), 4.03-4.05(t, 4H, Ar-OCH_2-), 4.11-4.15(t, 4H, Ar-O-CH_2-), 6.94(d, 2H, J = 2 Hz, Ar-H), 6.95(d, 2H, J = 2 Hz, Ar-H), 7.02(d, 2H, J = 2.4 Hz, Ar-H), 7.05(d, 2H, J = 2 Hz, Ar-H), 7.84(d, 2H, J = 2.8 Hz, Ar-H), 7.88(d, 2H, J = 4.8 Hz, Ar-H), 8.10(d, 2H, J = 2.8 Hz, Ar-H), 8.04(d, 2H, J = 2.8 Hz, Ar-H), 8.72, 8.91(s, 2H, -CH=N-). **^{13}C NMR** (100 MHz, $CDCl_3$): δc 10.45, 10.50 ($-CH_3$), 22.42, 22.50, 25.85, 25.91, for methylene carbons ($-CH_2-CH_2-$), 67.78, 67.82, 67.90, 69.75 (Ar-OCH_2-), 114.20, 114.40, 114.70, 114.73, 114.80, 121.33, 122.23, 129.70, 129.80, 129.95, 132.05, 132.06, 132.34 for aromatic carbons, 163.67, 163.97 (-CH=N-), 171.39, 171.90 (-C=N- thiadiazole).

1,1'-((propane-1,3-diylbis(oxy))bis(4,1-phenylene))bis(N-(5-(4-butoxyphenyl)-1,3,4-thiadiazol-2-yl)methanimine) (5d)

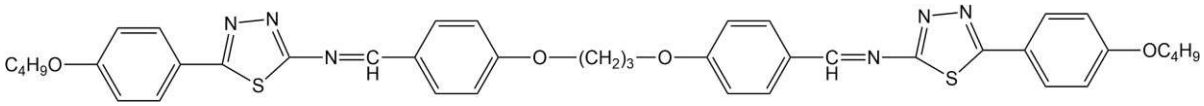

Creamy white crystalline solid**; IR** ν_{max} (KBr, cm^{-1}) 2956, 2930, 2875 (ν C-H aliphatic), 1605 (ν C=N), 1577, 1509, 1465, 1450, 1427 (ν C=C aromatic), 1253 (ν Ar-O-R), 1171, 1158, 1123, 1111 (ν C-N), 696 (ν C-S-C). **^{1}H NMR** (400 MHz, $CDCl_3$, TMS) δ_H 0.98-1.03(t, 6H, $-CH_3$), 1.48-1.76(m, 8H, $-CH_2-CH_2-$), 1.80-1.83(m, 2H, $-CH_2-CH_2-$), 4.01-4.05(t, 4H, Ar-OCH_2-), 4.11-4.15(t, 4H, Ar-O-CH_2-), 6.93(d, 2H, J = 2 Hz, Ar-H), 6.94(d, 2H, J = 4.8 Hz, Ar-H), 7.02(d, 2H, J = 2 Hz, Ar-H), 7.04(d, 2H, J = 5.2 Hz, Ar-H), 7.88(d, 2H, J = 2 Hz Ar-H), 7.85(d, 2H, J = 1.6 Hz, Ar-H), 8.04(d, 2H, J = 2 Hz, Ar-H), 8.04(d, 2H, J = 5.2 Hz, Ar-H), 8.60, 8.90(s, 2H, -CH=N-). **^{13}C NMR** (100 MHz, $CDCl_3$) δc 13.84, 14.82 ($-CH_3$), 19.11, 19.22 ($-CH_2-CH_3$), 25.88, 25.91, 31.11, 31.14, for methylene carbons ($-CH_2-CH_2-$), 67.79, 67.83, 68.92, 69.86 (Ar-OCH_2-), 114.20, 114.23, 114.30, 114.40, 114.60, 114.73, 121.32, 121.60, 122.21, 122.22, 122.50, 122.60, 129.98, 130.10, 132.06, 132.33 for aromatic carbons, 163.67, 163.97 (-CH=N-), 171.25, 171.30 (-C=N- thiadiazole).

1,1'-((propane-1,3-diylbis(oxy))bis(4,1-phenylene))bis(N-(5-(4-pentyloxyphenyl)-1,3,4-thiadiazol-2-yl)methanimine) (5e)

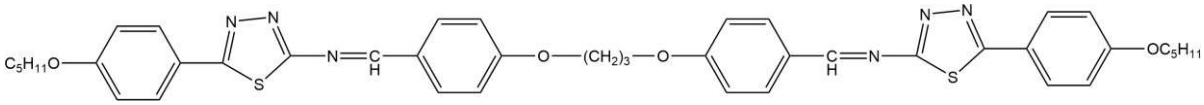

White crystalline solid**; IR** ν_{max} (KBr, cm^{-1}) 2954, 2933, 2870, 2855 (ν C-H aliphatic), 1606 (ν C=N), 1578, 1509, 1469, 1430 (ν C=C aromatic), 1259 (ν Ar-O-R), 1169 (ν C-N), 696 (ν C-S-C). **^{1}H NMR** (400 MH_Z, $CDCl_3$, TMS) δ_H 0.94-0.99(t, 6H, $-CH_3$), 1.41-1.43(m, 4H, $-CH_2-CH_2-$), 1.44-1.46(m, 4H, $-C\underline{H}_2-CH_3$), 1.79(m, 2H, $-CH_2-CH_2-$), 1.81(m, 2H, $-CH_2-CH_2-$), 1.82-1.86(m, 2H, $-CH_2-CH_2-$), 4.01-4.05(t, 4H, Ar-OCH_2-), 4.06-4.12(t, 4H, Ar-O-CH_2-), 6.96(d, 2H, J = 2 Hz, Ar-H), 6.98(d, 2H, J = 2 Hz, Ar-H), 7.02(d, 2H, J = 1.6 Hz, Ar-H), 7.04(d, 2H, J = 5.2 Hz, Ar-H), 7.88(d, 2H, J = 2 Hz, Ar-H), 7.89(d, 2H, J = 1.6 Hz, Ar-H), 8.04(d, 2H, J = 2 Hz, Ar-H), 8.08(d, 2H, J = 4.8 Hz, Ar-H), 8.90, 8.99(s, 2H, -CH=N-). **^{13}C NMR** (100 MHz, $CDCl_3$) δc 14.04, 14.09 ($-CH_3$), 22.47, 22.49 ($-\underline{C}H_2-CH_3$), 28.12, 28.13, 28.80, 28.90, for methylene carbons ($-CH_2-CH_2-$), 67.76, 67.80, 68.28, 68.30 (Ar-OCH_2-), 114.20, 114.30, 114.42, 114.62, 114.73, 121.32, 121.41, 121.45, 121.46, 121.65, 122.21, 122.22, 122.50, 122.60, 129.80, 129.98, 130.10, 132.07, 132.34 for aromatic carbons, 163.67, 163.68 (-CH=N-), 171.38, 171.39 (-C=N- thiadiazole).

1,1'-((propane-1,3-diylbis(oxy))bis(4,1-phenylene))bis(N-(5-(4-hexyloxyphenyl)-1,3,4-thiadiazol-2-yl)methanimine) (5f)

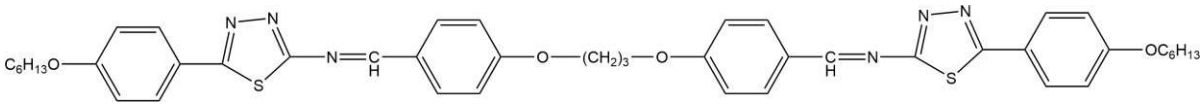

Pale yellow crystalline solid; **IR** ν_{max} (KBr, cm^{-1}) 2955, 2939, 2872, 2855, 2790, 2719 (ν C-H aliphatic), 1606 (ν C=N), 1581, 1513, 1449, 1445, 1429 (ν C=C aromatic), 1259 (ν Ar-O-R), 1606 (ν C-N), 696 (ν C-S-C). **^{1}H NMR** (400 MH_Z, $CDCl_3$, TMS) δ_H 0.89-0.92(t, 6H, $-CH_3$), 1.40-1.44(m, 8H, $-CH_2-CH_2-$), 1.44-1.46(m, 2H, $-C\underline{H}_2-CH_2-$), 1.79-1.82(m, 4H, $-CH_2-CH_2-$), 1.86-1.88(m, 4H, $-CH_2-CH_2-$), 4.02-4.06(t, 4H, Ar-O-CH_2-), 4.09-4.11(t, 4H, Ar-O-CH_2-), 7.03(d, 2H, J = 1.8 Hz, Ar-H), 7.04(d, 2H, J = 4 Hz, Ar-H), 7.06(d, 2H, J = 4 Hz, Ar-H), 7.09(d, 2H, J = 4 Hz, Ar-H), 7.88(d, 2H, J = 2 Hz, Ar-H), 7.88(d, 2H, J = 1.4 Hz Ar-H), 8.04(d, 2H, J = 4 Hz, Ar-H), 8.06(d, 2H, J = 4.4 Hz, Ar-H), 8.80, 8.90(s, 2H, -CH=N-). **^{13}C NMR** (100 MHz, $CDCl_3$) δc 14.02, 14.03 ($-CH_3$), 22.58, 22.60 ($-\underline{C}H_2-CH_3$), 25.09, 25.14, 28.91, 28.92, 29.15, 29.17, 31.11, 31.18 for methylene carbons ($-CH_2-CH_2-$), 67.78, 67.88, 68.30, 68.32 (Ar-OCH_2-

), 114.21, 114.31, 114.43, 114.66, 114.75, 114.29, 114.31, 121.30, 121.35, 121.60, 121.65, 122.21, 122.24, 122.50, 122.60, 129.80, 129.98, 130.10, 132.07, 132.34 for aromatic carbons, 163.70, 163.72 (-CH=N-), 171.40, 171.44 (-C=N- thiadiazole).

1,1'-((propane-1,3-diylbis(oxy))bis(4,1-phenylene))bis(N-(5-(4-heptyloxyphenyl)-1,3,4-thiadiazol-2-yl)methanimine) (5g)

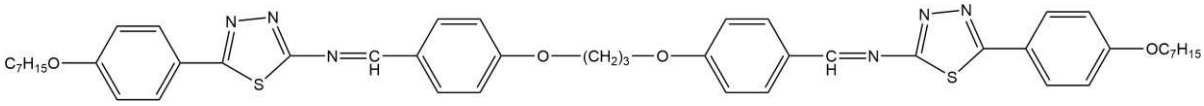

Off-white crystalline solid; **IR** ν_{max} (KBr, cm^{-1}) 2951, 2936, 2851, 2794 (ν C-H aliphatic), 1607 (ν C=N), 1578, 1509, 1467, 1429 (ν C=C aromatic), 1258 (ν Ar-O-R), 1172, 1165 (ν C-N), 696 (ν C-S-C). **^{1}H NMR** (400 MH_Z, $CDCl_3$, TMS) δ_H 0.88-0.92(t, 6H, $-CH_3$), 1.30-1.38(m, 14H, $-CH_2-CH_2-$), 1.78-1.83(m, 4H, $-CH_2-CH_2-$), 1.81-1.86(m, 4H, $-CH_2-CH_2-$), 4.01-4.04(t, 4H, Ar-O-CH_2-), 4.12-4.18(t, 4H, Ar-O-CH_2-), 6.96(d, 2H, J = 2 Hz, Ar-H), 6.92(d, 2H, J = 4.8 Hz, Ar-H), 7.04(d, 2H, J = 1.6 Hz, Ar-H), 7.01(d, 2H, J = 5.2 Hz, Ar-H), 7.84(d, 2H, J = 2 Hz, Ar-H), 7.88(d, 2H, J = 5.2 Hz, Ar-H), 8.02(d, 2H, J = 2 Hz, Ar-H), 8.06(d, 2H, J = 5.2 Hz, Ar-H), 8.70, 8.90(s, 2H, -CH=N-). **^{13}C NMR** (100 MHz, $CDCl_3$): δc 14.10, 14.18 ($-CH_3$), 22.61, 22.62 ($-\underline{C}H_2-CH_3$), 25.81, 25.85, 25.95, 25.96, 29.04, 29.06, 29.10, 29.20, 31.77, 31.81 for methylene carbons ($-CH_2-CH_2-$), 67.76, 67.78, 68.30, 68.32 (Ar-OCH_2-), 114.20, 114.22, 114.32, 114.52, 114.72, 114.73, 114.30, 114.31, 121.36, 121.38, 121.40, 121.60, 122.21, 122.24, 122.40, 122.62, 129.82, 129.90, 132.06, 132.10, 132.34 for aromatic carbons, 163.68, 163.97 (-CH=N-), 171.36, 171.38 (-C=N- thiadiazole).

1,1'-((propane-1,3-diylbis(oxy))bis(4,1-phenylene))bis(N-(5-(4-octyloxyphenyl)-1,3,4-thiadiazol-2-yl)methanimine) (5h)

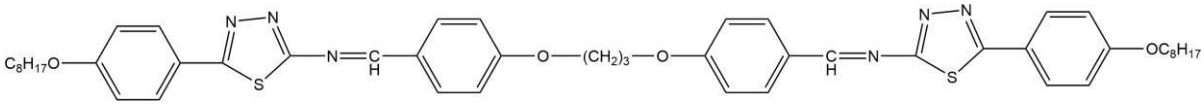

Off-white crystalline solid; **IR** ν_{max} (KBr, cm^{-1}) 2951, 2924, 2851 (ν C-H aliphatic), 1605 (ν C=N), 1575, 1509, 1468, 1429 (ν C=C aromatic), 1256 (ν Ar-O-R), 1166 (ν C-N), 697 (ν C-S-C). **^{1}H NMR** (400 MH_Z, $CDCl_3$, TMS) δ_H 0.87-0.91(t, 6H, $-CH_3$), 1.30-1.39(m, 24H, $-CH_2-CH_2-$), 1.78-1.82(m, 2H, $-CH_2-CH_2-$), 4.04-4.07(t, 4H, Ar-O-CH_2-), 4.12-4.18(t, 4H, Ar-O-CH_2-), 6.96(d, 2H, J = 2 Hz, Ar-H), 6.98(d, 2H, J = 4.8 Hz, Ar-H) 7.02(d, 2H, J = 1.6 Hz, Ar-H), 7.03(d, 2H, J = 5.2 Hz, Ar-H), 7.86(d, 2H, J = 2 Hz, Ar-H), 7.88(d, 2H, J = 4.8 Hz, Ar-H),

8.05(d, 2H, *J* = 2 Hz, Ar-H), 8.07(d, 2H, *J* = 5.2 Hz, Ar-H), 8.91, 8.99(s, 2H, -CH=N-). **^{13}C NMR** (100 MHz, $CDCl_3$): δc 14.12, 14.14 (-CH_3), 22.67, 22.68 (-$\underline{C}H_2$-CH_3), 25.81, 25.99, 29.10, 29.20, 29.23, 29.30, 29.33, 29.38, 31.81, 31.84 for methylene carbons (-CH_2-CH_2-), 67.74, 67.5, 67.76, 68.31 (Ar-OCH_2-), 114.20, 114.24, 114.28, 114.30, 114.34, 114.38, 114.40, 114.41, 114.73, 121.36, 121.39, 121.42, 121.65, 122.41, 122.42, 122.44, 122.60, 129.82, 129.95, 132.07, 132.34 for aromatic carbons, 163.69, 163.98 (-CH=N-), 171.69, 171.70 (-C=N- thiadiazole).

1,1'-((propane-1,3-diylbis(oxy))bis(4,1-phenylene))bis(N-(5-(4-decyloxyphenyl)-1,3,4-thiadiazol-2-yl)methanimine) (5i)

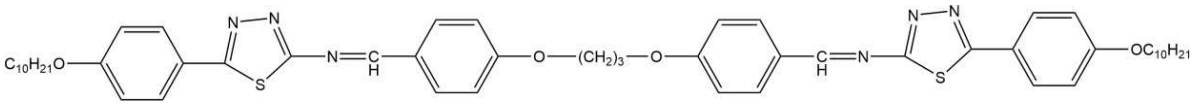

Light yellow crystalline solid**; IR** ν_{max} (KBr, cm^{-1}) 2924, 2870, 2851 (*ν* C-H aliphatic), 1605 (*ν* C=N), 1579, 1512, 1470, 1429 (*ν* C=C aromatic), 1257 (*ν* Ar-O-R), 1171 (*ν* C-N), 694 (*ν* C-S-C). **^{1}H NMR** (400 MH_Z, $CDCl_3$, TMS) δ_H 0.89-0.94(t, 6H, -CH_3), 1.24-1.81(m, 32H, -CH_2-CH_2-), 1.82-1.86(m, 2H, -CH_2-CH_2-), 4.01-4.06(t, 4H, Ar-O-CH_2-), 4.21-4.27(t, 4H, Ar-O-CH_2-), 7.05(d, 2H, *J* = 8.8 Hz, Ar-H), 7.06(d, 2H, *J* = 5.2 Hz, Ar-H), 7.86(d, 2H, *J* = 2.4 Hz, Ar-H), 7.88(d, 2H, *J* = 5.2 Hz, Ar-H), 7.89(d, 2H, *J* = 1.6 Hz, Ar-H), 8.01(d, 2H, *J* = 2.8 Hz, Ar-H), 8.03(d, 2H, *J* = 1.6 Hz, Ar-H), 8.06(d, 2H, *J* = 5.2 Hz, Ar-H), 8.80, 8.91(s, 2H, -CH=N-). **^{13}C NMR** (100 MHz, $CDCl_3$): δc 14.13, 14.14 (-CH_3), 22.69, 22.70 (-$\underline{C}H_2$-CH_3), 25.81, 25.84, 25.98, 25.99, 29.09, 29.10, 29.23, 29.30, 29.33, 29.36, 29.40, 29.46, 29.56, 31.90 for methylene carbons (-CH_2-CH_2-), 67.76, 67.78, 67.30, 68.32 (Ar-OCH_2-), 114.20, 114.22, 114.30, 114.38, 114.42, 114.44, 114.73, 121.30, 121.36, 121.38, 121.70, 122.45, 122.48, 122.49, 129.96, 132.06, 132.33 for aromatic carbons, 163.67, 163.97 (-CH=N-), 171.24, 171.30 (-C=N- thiadiazole).

1,1'-((propane-1,3-diylbis(oxy))bis(4,1-phenylene))bis(N-(5-(4-dodecyloxyphenyl)-1,3,4-thiadiazol-2-yl)methanimine) (5j)

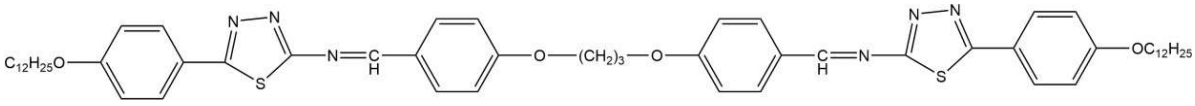

Creamy white crystalline solid; **IR** ν_{max} (KBr, cm^{-1}) 2919, 2848 (*ν* C-H aliphatic), 1605 (*ν* C=N), 1579, 1510, 1467, 1428 (*ν* C=C aromatic), 1256 (*ν* Ar-O-R), 1172 (*ν* C-N), 695 (*ν* C-S-C). **^{1}H NMR** (400 MH_Z, $CDCl_3$, TMS) δ_H 0.86-0.91(t, 6H, -CH_3), 1.26-1.38(m, 20H, -CH_2-

CH_2-), 1.40-1.81(m, 20H, -CH_2-CH_2-), 1.81-1.86(m, 2H, -CH_2-CH_2-), 4.01-4.08(t, 4H, Ar-O-CH_2-), 4.12-4.18(t, 4H, Ar-O-CH_2-), 6.96(d, 2H, *J* = 2.4 Hz, Ar-H), 6.97(d, 2H, *J* = 4.8 Hz, Ar-H), 7.02(d, 2H, *J* = 1.6 Hz, Ar-H), 7.03(d, 2H, *J* = 5.2 Hz, Ar-H), 7.87(d, 2H, *J* = 4.8 Hz, Ar-H), 7.88(d, 2H, *J* = 4.8 Hz, Ar-H), 8.02(d, 4H, *J* = 2 Hz, Ar-H), 8.89, 8.99(s, 2H, -CH=N-). **^{13}C NMR** (100 MHz, $CDCl_3$): δc 14.14, 14.16 (-CH_3), 22.71, 22.72 (-CH_2-CH_3), 25.81, 25.82, 25.98, 25.99, 29.09, 29.11, 29.36, 29.38, 29.57, 29.58, 29.60, 29.62, 29.65, 29.66, 29.67, 29.68, 30.96, 30.98, 31.93, 31.96 for methylene carbons (-CH_2-CH_2-), 67.76, 67.79, 68.30, 68.34 (Ar-OCH_2-), 114.20, 114.22, 114.30, 114.32, 114.36, 114.38, 114.40, 114.42, 114.44, 114.46, 114.70, 114.73, 121.32, 121.34, 121.36, 121.38, 122.42, 122.46, 122.48, 129.96, 132.05, 132.33 for aromatic carbons, 163.67, 163.97 (-CH=N-), 170.40, 171.01 (-C=N- thiadiazole).

1,1'-((propane-1,3-diylbis(oxy))bis(4,1-phenylene))bis(N-(5-(4-tetradecyloxyphenyl)-1,3,4-thiadiazol-2-yl)methanimine) (5k)

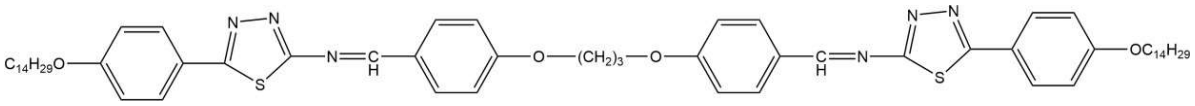

Pale yellow crystalline solid; **IR** ν_{max} (KBr, cm^{-1}) 2922, 2858 (*v* C-H aliphatic), 1609 (*v* C=N), 1575, 1518, 1467, 1431 (*v* C=C aromatic), 1258 (*v* Ar-O-R), 1178 (*v* C-N), 695 (*v* C-S-C). **^{1}H NMR** (400 MH_Z, $CDCl_3$, TMS) δ_H 0.88-0.93(t, 6H, -CH_3), 1.24-1.36(m, 24H, -CH_2-CH_2-), 1.34-1.41(m, 24H, -CH_2-CH_2-), 1.84-1.89(m, 2H, -CH_2-CH_2-), 4.02-4.06(t, 4H, Ar-O-CH_2-), 4.18-4.26(t, 4H, Ar-O-CH_2-), 7.02(d, 2H, *J* = 2.4 Hz, Ar-H), 7.03(d, 2H, *J* = 4.8 Hz, Ar-H), 7.04(d, 2H, *J* = 1.6 Hz, Ar-H), 7.06(d, 2H, *J* = 5.2 Hz, Ar-H), 7.86(d, 2H, *J* = 4.8 Hz, Ar-H), 7.88(d, 2H, *J* = 4.8 Hz, Ar-H), 8.06(d, 2H, *J* = 2 Hz, Ar-H), 8.07(d, 2H, *J* = 5.2 Hz, Ar-H), 8.90, 8.99(s, 2H, -CH=N-). **^{13}C NMR** (100 MHz, $CDCl_3$): δc 14.15, 14.17 (-CH_3), 22.71, 22.73 (-CH_2-CH_3), 25.99, 28.97, 28.99, 29.10, 29.20, 29.38, 29.40, 29.57, 29.60, 29.62, 29.67, 29.69, 29.70, 29.71, 29.72, 31.94 for methylene carbons (-CH_2-CH_2-), 63.53, 64.52, 68.20, 67.79, 68.30 (Ar-OCH_2-), 114.20, 114.22, 114.30, 114.33, 114.35, 114.39, 114.42, 114.42, 114.44, 114.46, 114.70, 114.72, 121.32, 121.33, 121.38, 121.39, 122.44, 122.46, 122.48, 129.96, 130.09, 132.06, 132.33 for aromatic carbons, 163.67, 163.77 (-CH=N-), 171.15, 171.18 (-C=N- thiadiazole).

1,1'-((propane-1,3-diylbis(oxy))bis(4,1-phenylene))bis(N-(5-(4-hexadecyloxyphenyl)-1,3,4-thidiazol-2-yl)methanimine) (5l)

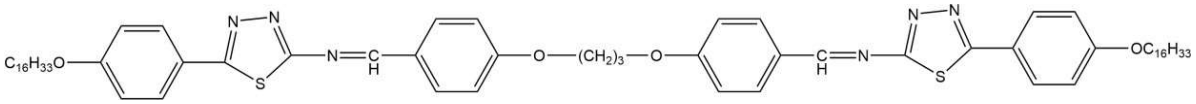

Light yellow crystalline solid; **IR** ν_{max} (KBr, cm^{-1}) 2929, 2821 (ν C-H aliphatic), 1606 (ν C=N), 1576, 1521, 1479, 1429 (ν C=C aromatic), 1250 (ν Ar-O-R), 1179 (ν C-N), 695 (ν C-S-C). **^{1}H NMR** (400 MHz, $CDCl_3$, TMS) δ_H 0.88-0.94(t, 6H, $-CH_3$), 1.26-1.40(m, 28H, $-CH_2-CH_2-$), 1.41-1.49(m, 28H, $-CH_2-CH_2-$), 1.85-1.89(m, 2H, $-CH_2-CH_2-$), 4.01-4.07(t, 4H, Ar-O-CH_2-), 4.08-4.22(t, 4H, Ar-O-CH_2-), 7.02(d, 2H, J = 2 Hz, Ar-H), 7.04(d, 2H, J = 4.2 Hz, Ar-H), 7.06(d, 2H, J = 1.6 Hz, Ar-H), 7.08(d, 2H, J = 5.2 Hz, Ar-H), 7.88(d, 2H, J = 4.2 Hz, Ar-H), 7.89(d, 2H, J = 4.8 Hz, Ar-H), 8.06(d, 2H, J = 2 Hz, Ar-H), 8.08(d, 2H, J = 5.2 Hz, Ar-H), 8.92, 8.99(s, 2H, -CH=N-). **^{13}C NMR** (100 MHz, $CDCl_3$: δc 14.13, 14.14 ($-CH_3$), 22.70, 22.71 ($-CH_2-CH_3$), 25.81, 25.82, 25.98, 25.98, 29.10, 29.12, 29.36, 29.38, 29.57, 29.58, 29.60, 29.62, 29.65, 29.66, 29.67, 29.68, 30.96, 30.98, 31.93, 31.96 for methylene carbons ($-CH_2-CH_2-$), 67.76, 67.79, 68.30, 68.34 (Ar-OCH_2-), 114.20, 114.22, 114.30, 114.32, 114.36, 114.38, 114.40, 114.42, 114.44, 114.46, 114.70, 114.73, 121.32, 121.34, 121.36, 121.38, 122.42, 122.46, 122.48, 129.96, 132.05, 132.33 for aromatic carbons, 163.67, 163.97 (-CH=N-), 170.40, 171.01 (-C=N- thiadiazole).

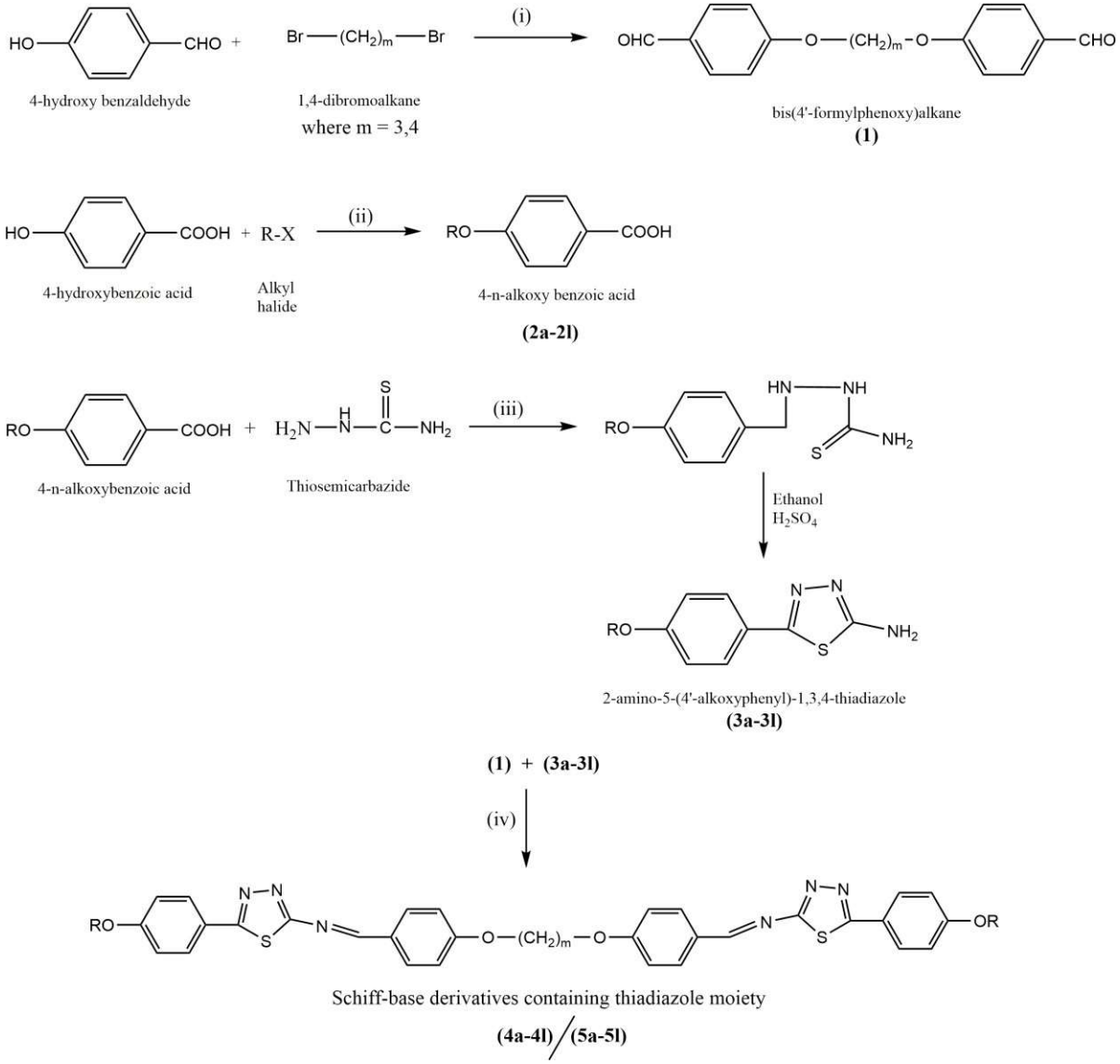

For m = 4 indicates (4a-4l) series-I, where R = -C_nH_{2n+1}, where n = 1-8, 10, 12, 14, 16

For m = 3 indicates (5a-5l) series-II, where R = -C_nH_{2n+1}, where n = 1-8, 10, 12, 14, 16.

Scheme 2.1: The synthetic procedure of thiadiazole-based homologous series-I & II **[(4a-4l) and (5a-5l)]**. Reagents and conditions: (i) anhydrous K_2CO_3, dry acetone, reflux 4-6 h; (ii) RBr, KOH, EtOH, reflux 8-10 h; (iii) Few drops of conc. H_2SO_4, EtOH, reflux 4 h; (iv)Few drops of glacial AcOH, absolute EtOH, reflux 3-4 h.

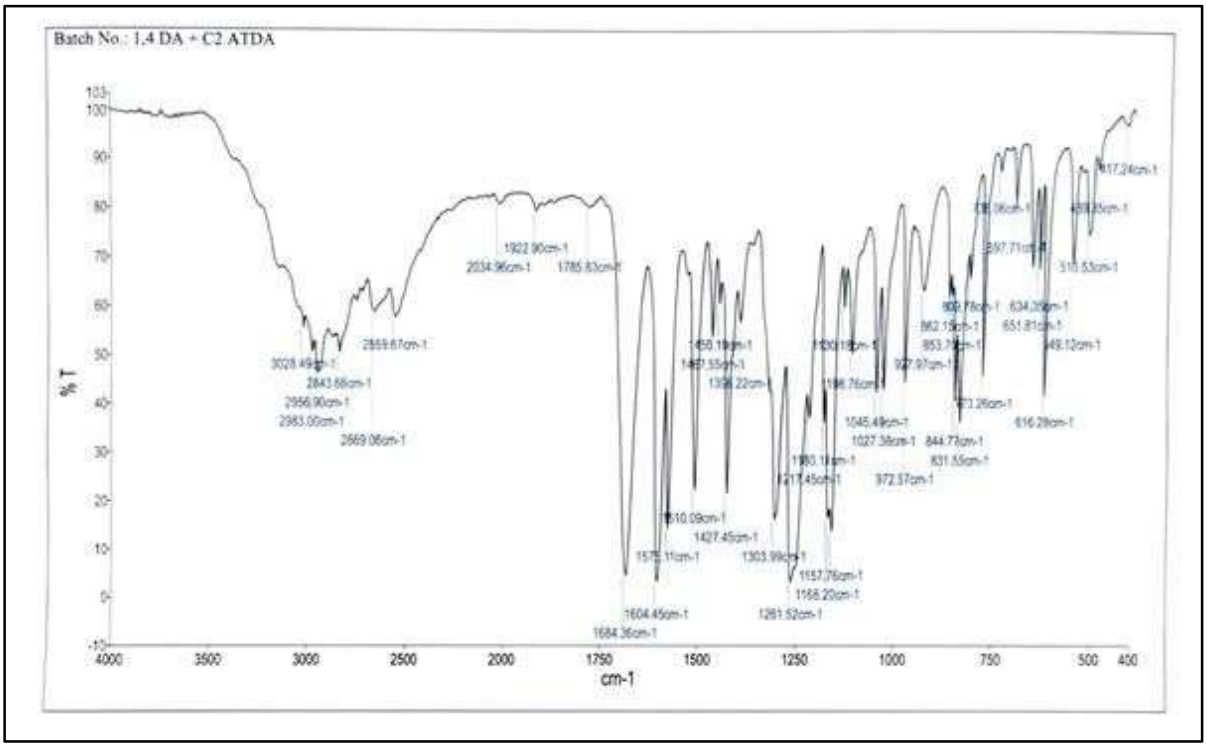

Figure 2.5: FT-IR spectra of 1,1'-(butane-1,4-diylbis(oxy))bis(4,1-phenylene))bis(N-5-(4-methoxyphenyl)-1,3,4-thiadiazol-2-yl)methanimine) (4a)

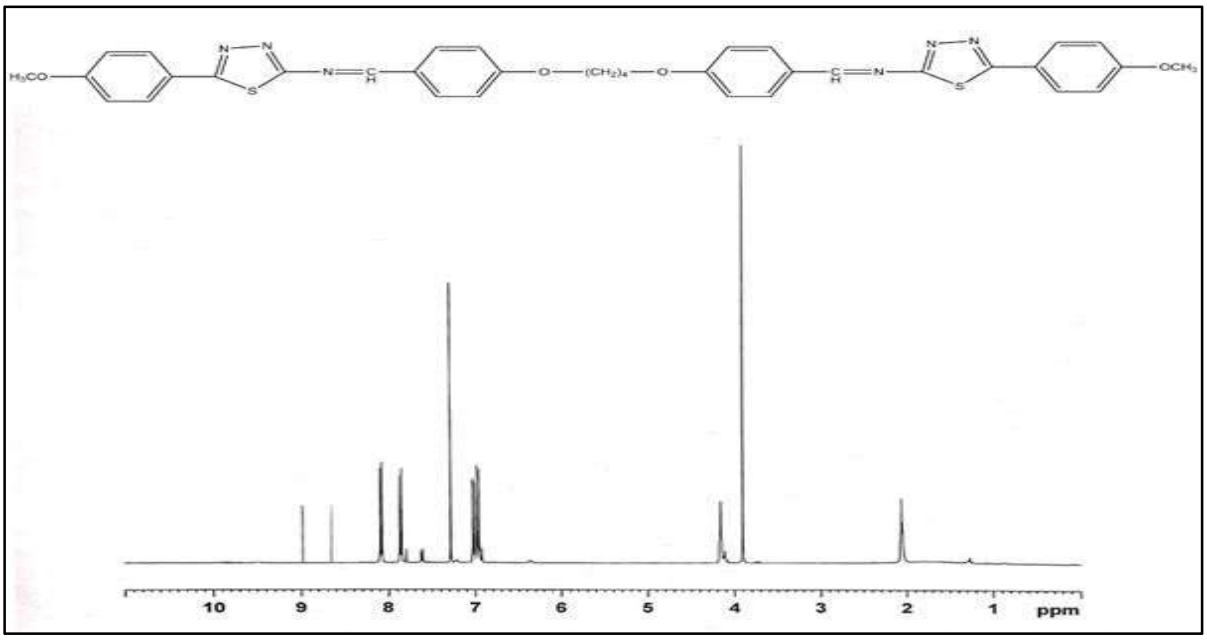

Figure 2.6: ^{1}H NMR spectra of 1,1'-(butane-1,4-diylbis(oxy))bis(4,1-phenylene))bis(N-5-(4-methoxyphenyl)-1,3,4-thiadiazol-2-yl)methanimine) (4a)

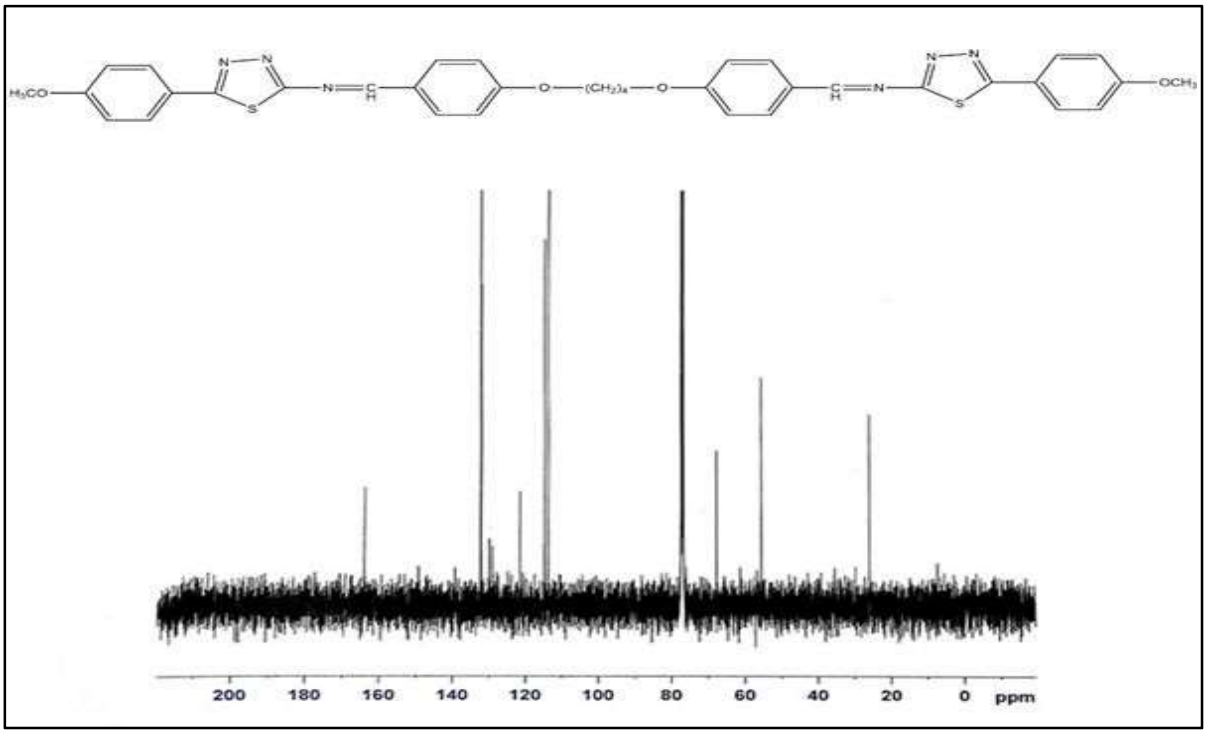

Figure 2.7: ^{13}C NMR spectra of 1,1'-(butane-1,4-diylbis(oxy))bis(4,1-phenylene))bis(N-5-(4-methoxyphenyl)-1,3,4-thiadiazol-2-yl)methanimine) (4a)

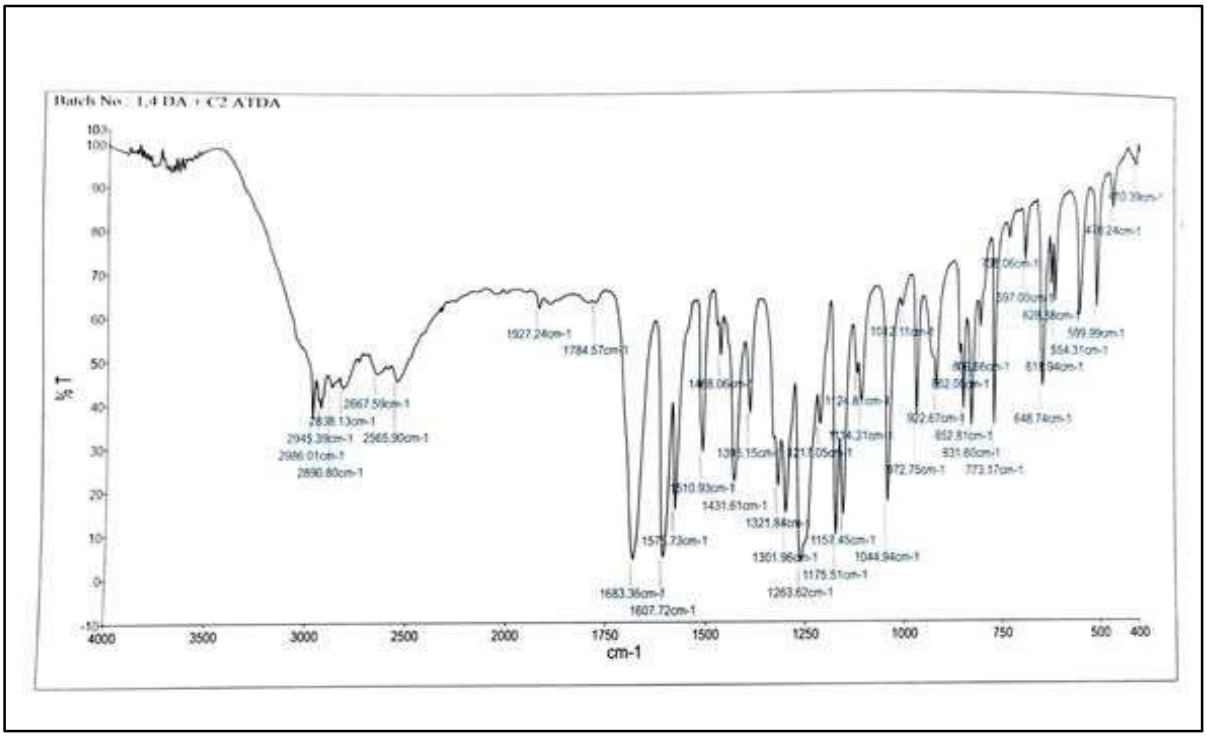

Figure 2.8: FT-IR spectra of 1,1'-(butane-1,4-diylbis(oxy))bis(4,1-phenylene))bis(N-5-(4-ethoxyphenyl)-1,3,4-thiadiazol-2-yl)methanimine) (4b)

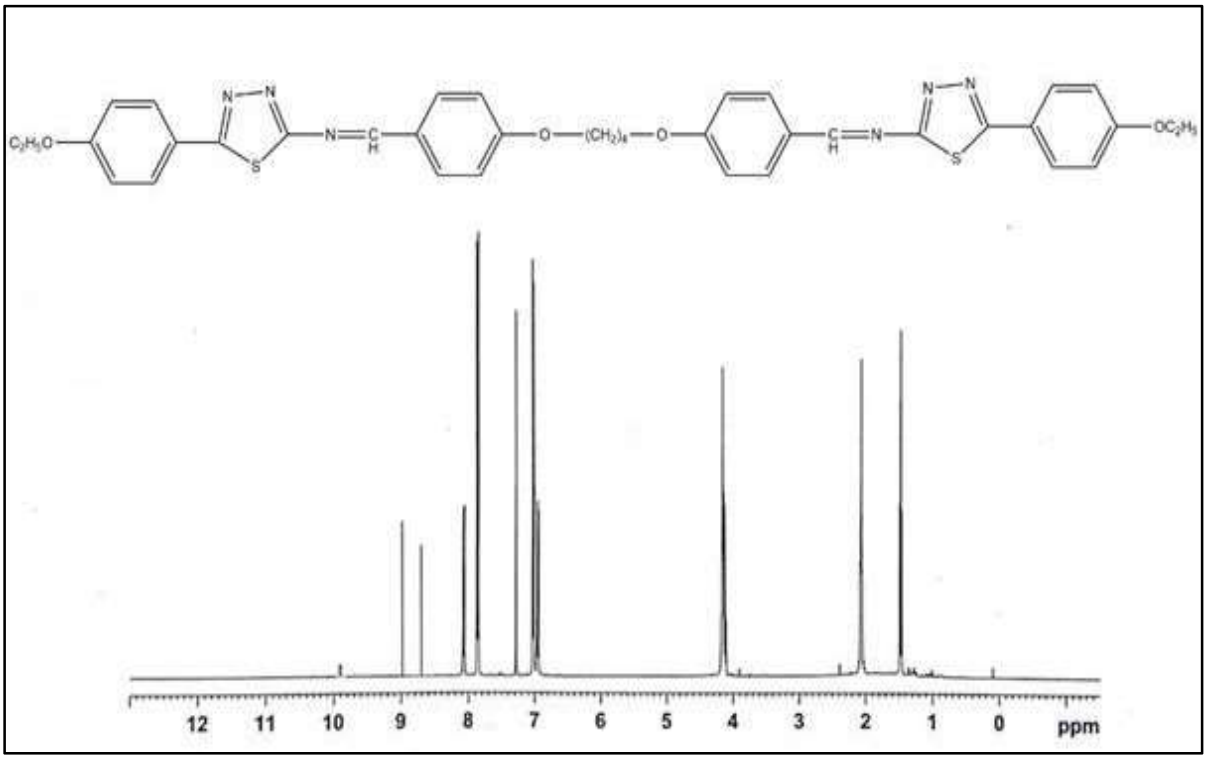

Figure 2.9: ^{1}H NMR of 1,1'-(butane-1,4-diylbis(oxy))bis(4,1-phenylene))bis(N-5-(4-ethoxyphenyl)-1,3,4-thiadiazol-2-yl)methanimine) (4b)

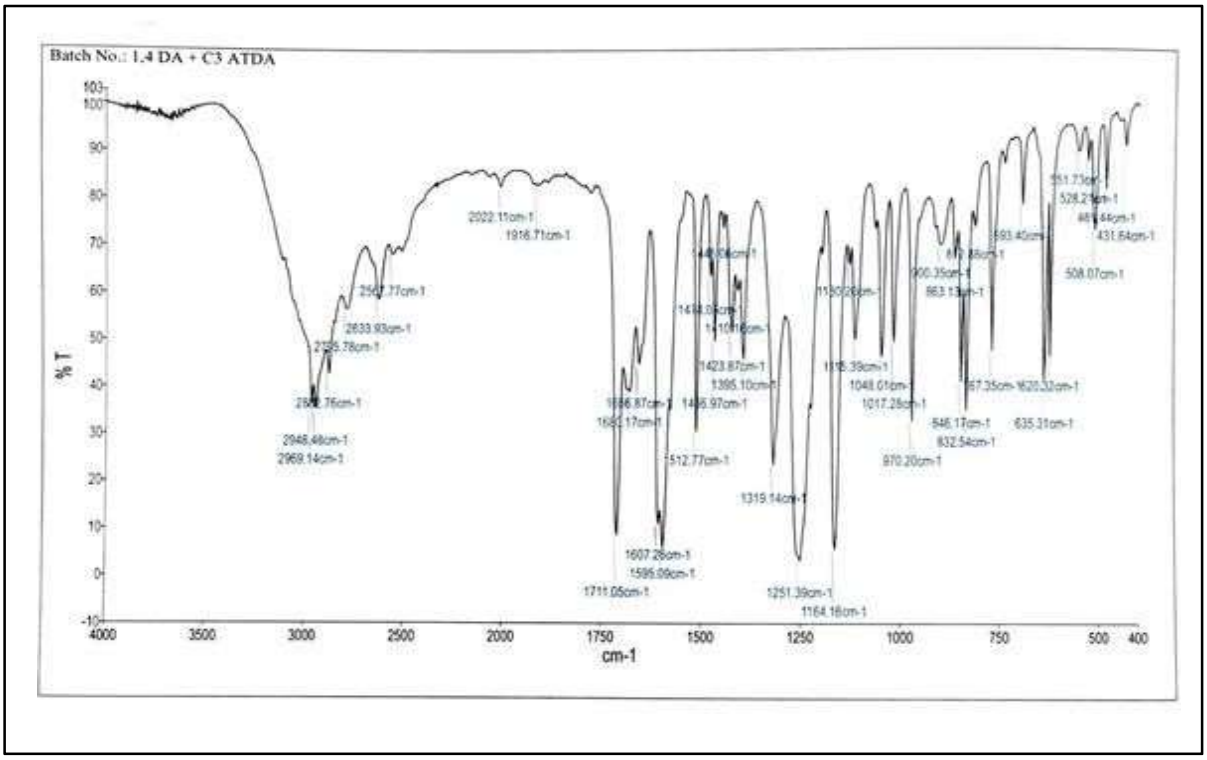

Figure 2.10: FT-IR spectra of 1,1'-(butane-1,4-diylbis(oxy))bis(4,1-phenylene))bis(N-5-(4-propoxyphenyl)-1,3,4-thiadiazol-2-yl)methanimine) (4c)

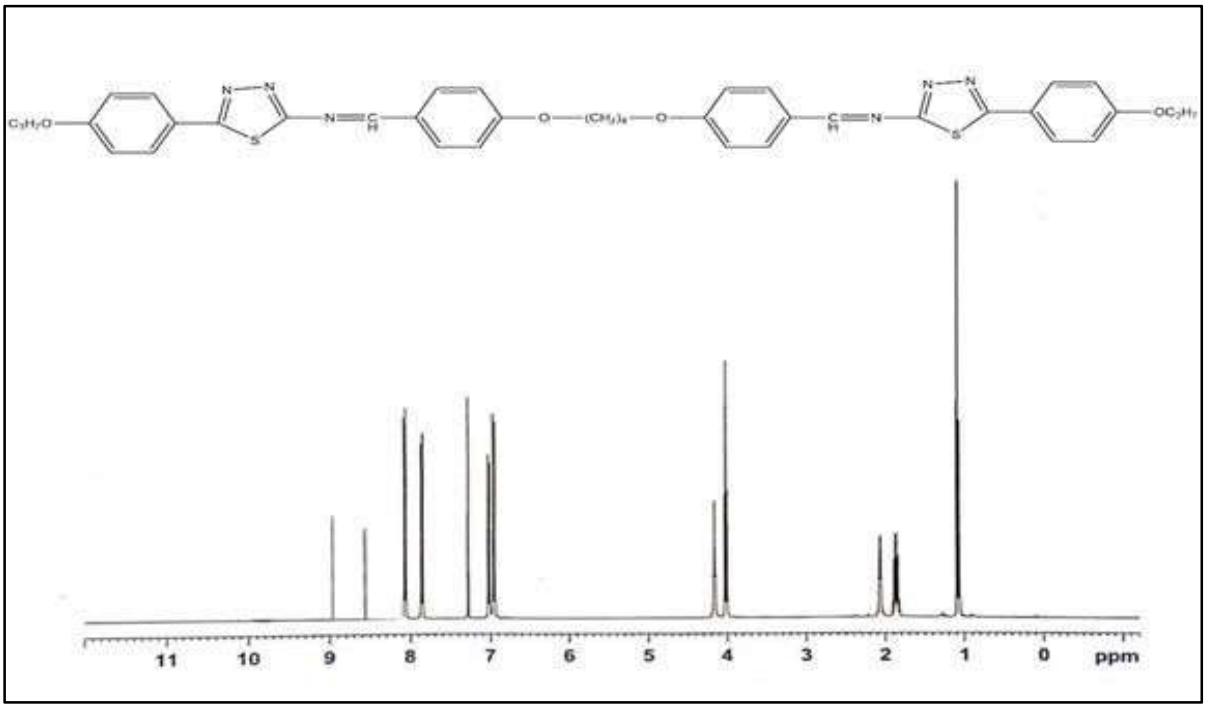

Figure 2.11: ^{1}H NMR of 1,1'-(butane-1,4-diylbis(oxy))bis(4,1-phenylene))bis(N-5-(4-propoxyphenyl)-1,3,4-thiadiazol-2-yl)methanimine) (4c)

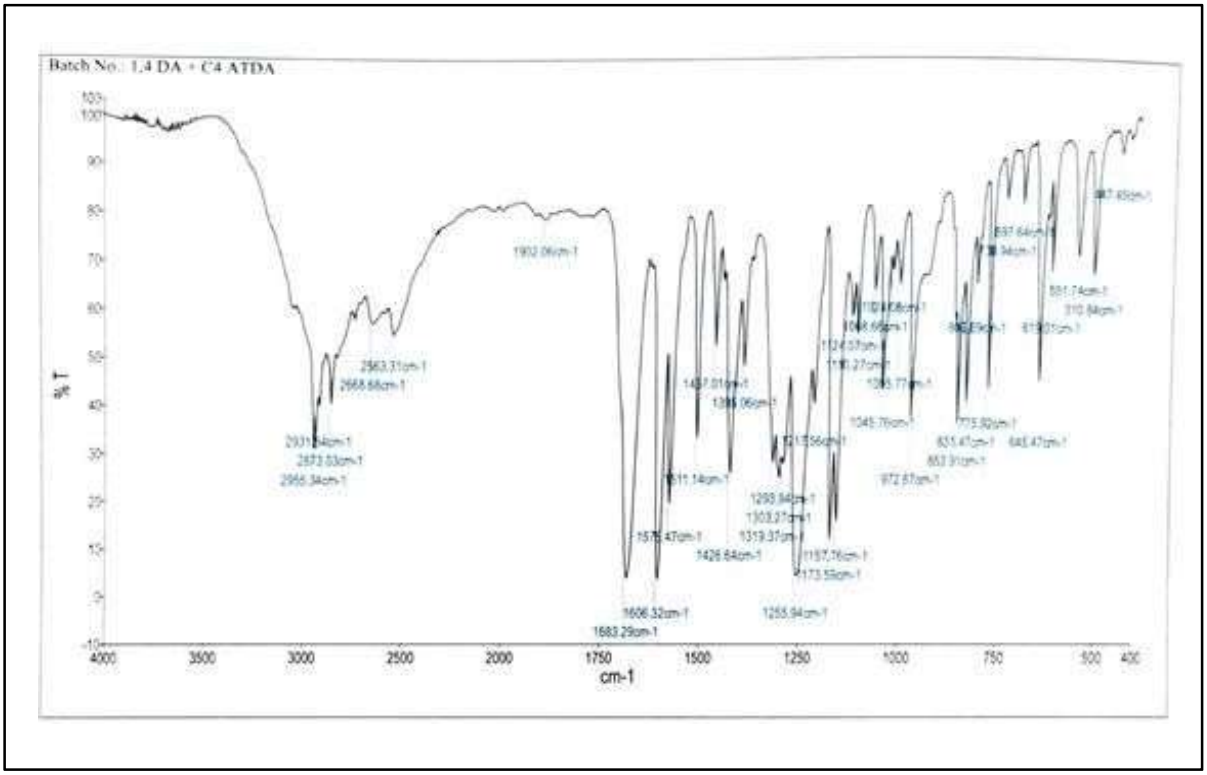

Figure 2.12: FT-IR spectra of 1,1'-(butane-1,4-diylbis(oxy))bis(4,1-phenylene))bis(N-5-(4-butoxyphenyl)-1,3,4-thiadiazol-2-yl)methanimine) (4d)

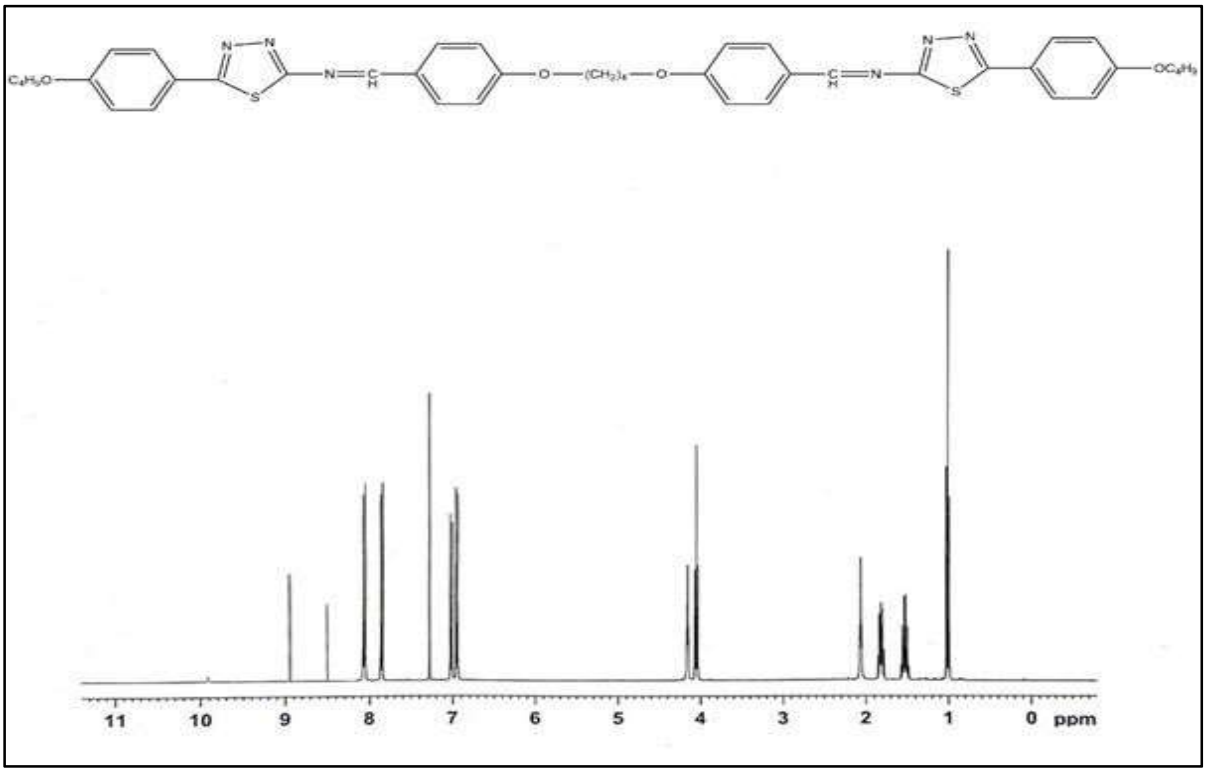

Figure 2.13: ^{1}H NMR of 1,1'-(butane-1,4-diylbis(oxy))bis(4,1-phenylene))bis(N-5-(4-butoxyphenyl)-1,3,4-thiadiazol-2-yl)methanimine) (4d)

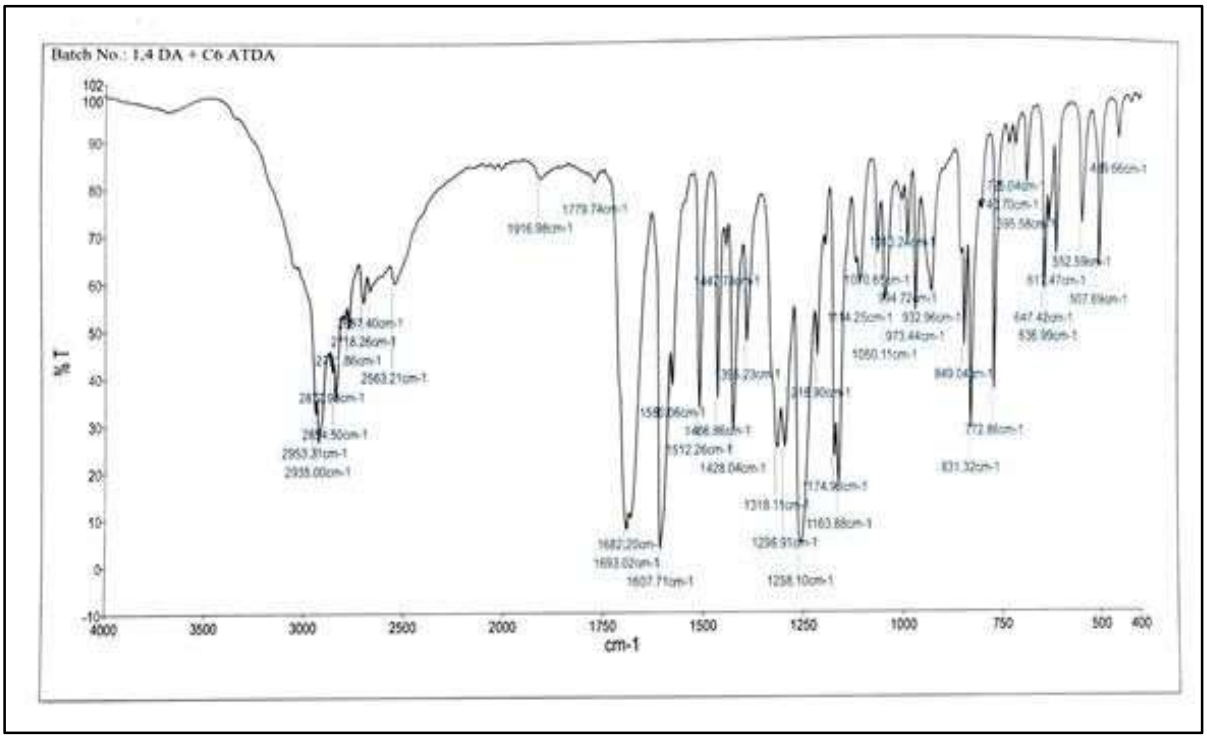

Figure 2.14: FT-IR spectra of 1,1'-(butane-1,4-diylbis(oxy))bis(4,1-phenylene))bis(N-5-(4-hexyloxyphenyl)-1,3,4-thiadiazol-2-yl)methanimine) (4f)

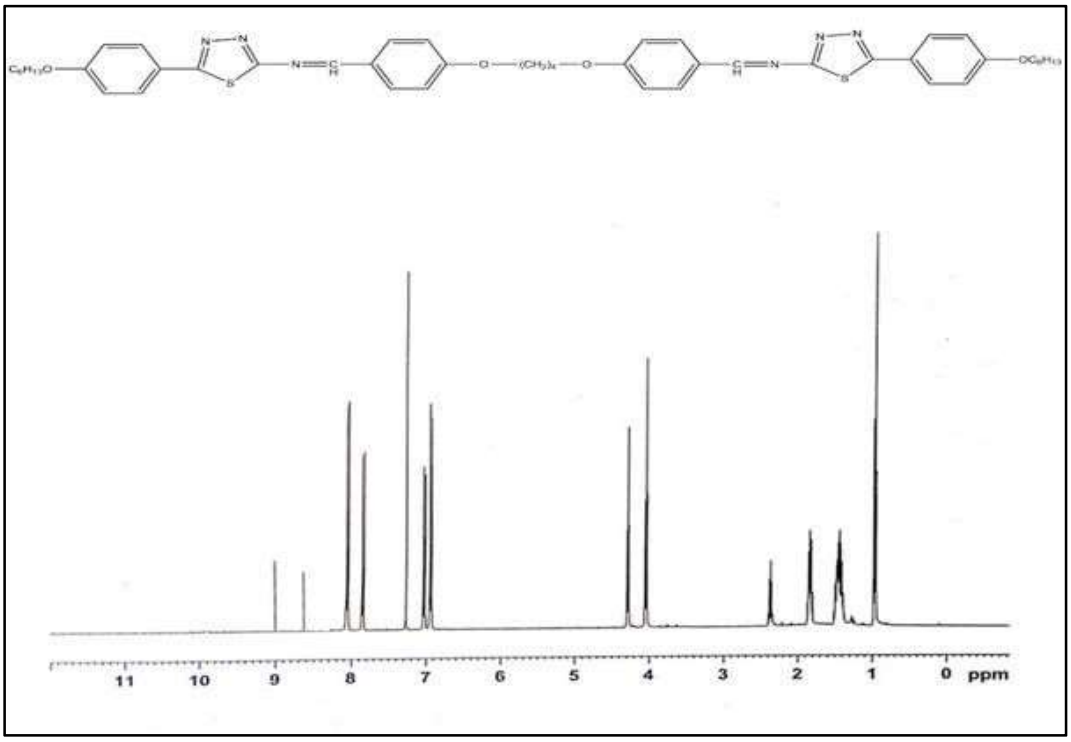

Figure 2.15: ^{1}H NMR of 1,1'-(butane-1,4-diylbis(oxy))bis(4,1-phenylene))bis(N-5-(4-hexyloxyphenyl)-1,3,4-thiadiazol-2-yl)methanimine) (4f)

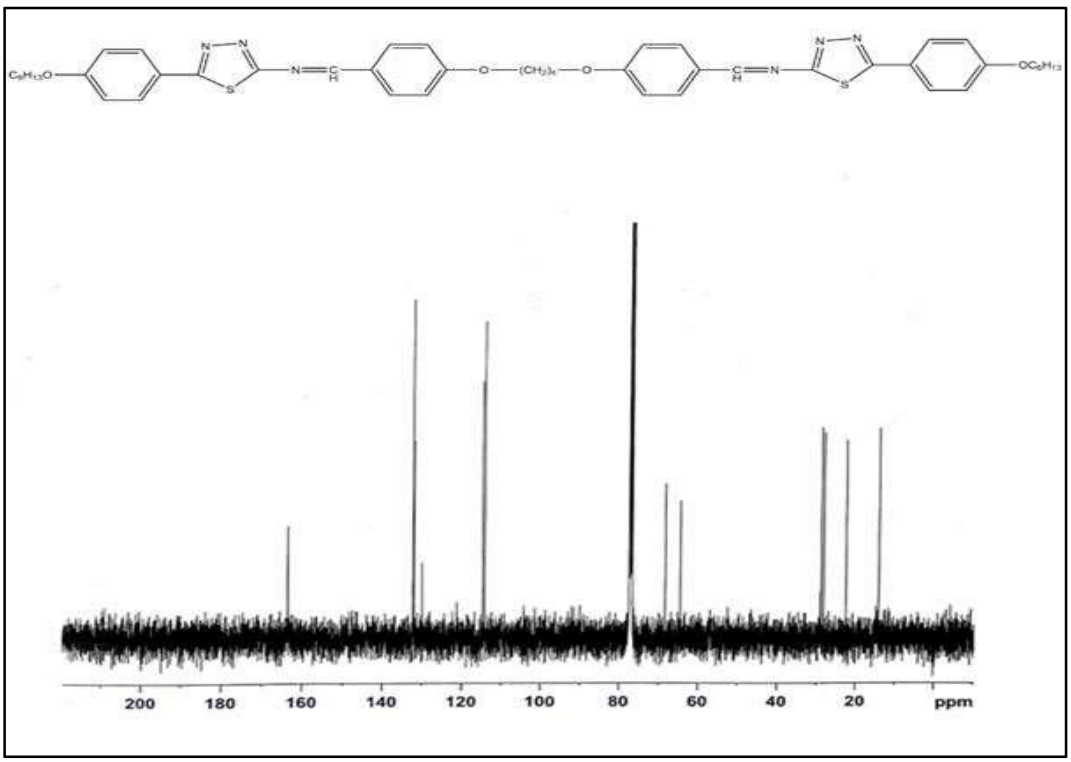

Figure 2.16: ^{13}C NMR of 1,1'-(butane-1,4-diylbis(oxy))bis(4,1-phenylene))bis(N-5-(4-hexyloxyphenyl)-1,3,4-thiadiazol-2-yl)methanimine) (4f)

Table 2.1: Physical data of series-I and II [(4a-4l) and (5a-5l)].

(4a-4l)

Compound code	n	Mol. Formula	% Yield	Elemental Analysis					
				Calculated (%)			Found (%)		
				C	H	N	C	H	N
4a	1	$C_{36}H_{32}N_6O_4S_2$	62.30	63.89	4.77	12.42	63.85	4.75	12.39
4b	2	$C_{38}H_{36}N_6O_4S_2$	75.11	64.75	5.15	11.92	64.72	5.12	11.90
4c	3	$C_{40}H_{40}N_6O_4S_2$	73.58	65.55	5.50	11.47	65.52	5.48	11.45
4d	4	$C_{42}H_{44}N_6O_4S_2$	68.15	66.29	5.83	11.04	66.25	5.80	11.01
4e	5	$C_{44}H_{48}N_6O_4S_2$	65.10	66.98	6.13	10.65	66.95	6.10	10.62
4f	6	$C_{46}H_{52}N_6O_4S_2$	82.48	67.72	6.42	10.29	67.60	6.40	10.25
4g	7	$C_{48}H_{56}N_6O_4S_2$	78.50	68.22	6.68	9.94	68.20	6.65	9.90
4h	8	$C_{50}H_{60}N_6O_4S_2$	81.06	68.78	6.93	9.62	68.75	6.90	9.60
4i	10	$C_{54}H_{68}N_6O_4S_2$	90.51	69.79	7.38	9.04	69.75	7.35	9.01
4j	12	$C_{58}H_{76}N_6O_4S_2$	92.73	70.70	7.77	8.53	70.68	7.74	8.51
4k	14	$C_{62}H_{84}N_6O_4S_2$	80.51	71.50	8.13	8.07	71.48	8.10	8.04
4l	16	$C_{66}H_{92}N_6O_4S_2$	73.33	73.33	8.45	7.66	73.30	8.42	7.62

(5a-5l)

Compound code	n	Mol. Formula	% Yield	Elemental Analysis					
				Calculated			Found		
				C	H	N	C	H	N
5a	1	$C_{35}H_{30}N_6O_4S_2$	62.60	63.43	4.56	12.68	63.40	4.51	12.65
5b	2	$C_{37}H_{34}N_6O_4S_2$	76.11	64.33	4.96	12.17	64.30	4.95	12.15
5c	3	$C_{39}H_{38}N_6O_4S_2$	74.68	65.16	5.33	11.69	65.11	5.31	11.67
5d	4	$C_{41}H_{42}N_6O_4S_2$	69.35	65.93	5.67	11.25	66.90	5.64	11.23
5e	5	$C_{43}H_{46}N_6O_4S_2$	68.40	66.64	5.98	10.84	66.68	5.95	10.82
5f	6	$C_{45}H_{50}N_6O_4S_2$	81.50	67.31	6.28	10.47	67.28	6.24	10.45
5g	7	$C_{47}H_{54}N_6O_4S_2$	79.40	67.92	6.55	10.11	67.90	6.53	10.09
5h	8	$C_{49}H_{58}N_6O_4S_2$	85.08	68.50	6.80	9.78	68.49	6.78	9.75
5i	10	$C_{53}H_{66}N_6O_4S_2$	89.49	69.55	7.27	9.18	69.52	7.25	9.15
5j	12	$C_{57}H_{74}N_6O_4S_2$	91.70	70.48	7.68	8.65	70.45	7.65	8.63
5k	14	$C_{61}H_{82}N_6O_4S_2$	81.50	71.31	8.04	8.18	71.32	8.01	8.15
5l	16	$C_{65}H_{90}N_6O_4S_2$	75.33	72.05	8.37	7.76	72.08	8.39	7.73

To determine the mesomorphic nature of the prepared compounds, the compounds were sandwiched between two untreated glass slides, and the microscopic textures and the transition temperatures were taken on heating and cooling cycles under an optical polarizing microscope. The stability of all the compounds was observed on repeated heating and cooling cycles.

The apparatus was verified by standardizing it with the known standards.

In series **(4a-4l)**, lower homologue starting from compounds **4a-4c** exhibit only nematic phase, whereas homologue from n-butyl to n-hexadecyl derivatives exhibit smectic and nematic phases in heating and cooling cycles.

Differential Scanning Calorimetry (DSC) was used to examine the transition temperatures, entropy change, and corresponding enthalpies. With indium serving as the reference, the device was calibrated. The related DSC thermograms and the phase transition temperatures recorded with a polarising optical microscope were found to be reasonably in accord.

2.3. Results and Discussion

The final Schiff's bases **(4a-4l) and (5a-5l)** were prepared by condensation of bis(4'-formylphenoxy)alkane **(1)** with the appropriate 2-amino-5-(4'-alkoxyphenyl)-1,3,4-thiadiazole **(3a-3l)**. The synthetic strategy for both prepared mesogenic compounds is depicted in Figure 2.1.

In the FT-IR spectra, (**4a-4l**) exhibit major IR bands between 2795-2986 cm^{-1} (ν C-H aliphatic), 1410-1595 cm^{-1} (ν C-C aromatic), 1251-1263 cm^{-1} (ν Ar-O-R) stretch. The appearance of a new band observed between 1604-1610 cm^{-1} corresponds to (ν C=N) which confirms the presence of azomethine group in the moiety. The absorption peak observed around 693-697 cm^{-1} represents (ν C-S-C).

Compounds in series (**4a–4l**) exhibited aromatic protons as a doublet with J values varying between δ 6.94–6.98, 7.01–7.88, and 8.01–8.09 ppm in ^{1}H-NMR. At δ 8.55-8.99 ppm, the imine protons (-CH=N-) were detected as a singlet. At δ 4.01-4.28 ppm, the alkoxy protons (-OCH_2-) exhibit a triplet and multiplet appearance due to their high degree of deshielding. The remaining alkoxy chain methylene protons (-CH_2-) have emerged as a multiplet with δ 1.25-1.89 ppm. At δ 0.89-1.47 ppm, a triplet of the terminal methyl group's protons is visible.

The imine carbon (-CH=N-) is represented by the peak between δ 163.43-164.0 ppm in the ^{13}C-NMR spectra of newly synthesised compounds from series I. The detected aromatic carbons ranged in δ from 113.76 to 132.36 ppm. The aromatic ring's methylene carbon was found to be linked to an alkoxy oxygen between δ 63.54-69.85 ppm. The remaining alkoxy chain methylene carbons were detected in the range of δ 19.10–31.96 ppm. The alkoxy chain's methyl carbon was found to be between δ 13.83 and 14.81 ppm.

All the members of the homologous series-I and II exhibit enantiotropic mesomorphic behaviour. In Series-I, lower homologues starting from (**4a-4c**) exhibit only the nematic phase, while higher homologues from n-butyl to n-hexadecyl derivatives exhibit smectic and nematic phases in heating as well as cooling cycles. In series-II, lower homologue starting from methyl to n-propyl derivatives (**5a-5c**) exhibit only nematic phase, while higher homologue from n-butyl to n-hexadecyl derivatives exhibit smectic and nematic phases in heating as well as cooling cycles. The transition temperatures are depicted in Table 2.2 and 2.4.

Alkoxy or alkyl chains are connected to one or both ends of the rather rigid aromatic or alicyclic rings that make up the molecules that form liquid crystals. The system's energy is determined by the many molecular conformations, steric repulsions between distinct molecules, and weak

chemical dispersive interactions between neighbouring molecules [70]. Grey [71, 72] has effectively applied the ideas on morphological orientation and interactions for the mesogenic homologous series. These ordering forces have to resist disordering thermal fluctuations and are highly dependent on molecule separations.

Mesogenic compounds melt gradually due to the lath-like molecules and balancing lateral and terminal cohesions. They transition into an isotropic liquid phase after going through one or more organized intermediate stages. The molecular layer structure of the smectic phase occurs in temperature intervals where molecular attractions prevail, while the similar molecular organisation of the nematic phase occurs at a temperature period with significant terminal attractions. Therefore, strong attractions are defeated at the Sm-N or Sm-N* change, and a nematic or chiral nematic mesophase is formed. At the crystal-smectic transition, the molecules principal terminal cohesions are overcome. The remaining terminal cohesions keep the molecules in either the nematic or chiral nematic mesophase.

The mesomorphic-isotropic transition temperatures in a homologous series varies uniquely. The transition temperatures of the series vary regularly due to the increment of each methylene unit. The behaviour has been described by Gray [73] by describing the terminal alkyl or alkoxy group's chain length. The strength of the terminal intermolecular cohesion should diminish as the alkoxy or alkyl chain lengthens since this will increase the spacing of the aromatic centers, which are highly polarisable and have permanent dipolar substituents. On the other hand, Gray [73] and Maier and Baumgartner [74] have proposed that the intermolecular attractions and the total polarizability of the molecules are both increased concurrently by the addition of each methylene unit. The lowest homologues in series-I and II are only nematic. Pure nematogens are found in the lower homologues where the terminal cohesions are highest and the aromatic nuclei are least separated. Since the lateral cohesive forces arise with terminal chain length and the molecules align themselves in the layered structure before transition to the nematic phase, the smectic phase dominates as we ascend the series from the middle members. Therefore, smectogenic mesophase should dominate at the expense of nematic phase stability. To sustain the parallel molecular orientation necessary for the nematic mesophase, the terminal intermolecular interactions are insufficient at this point. This is the typical pattern found in a typical homologous nematogenic sequence.

The variation of N-I transitions has been explained by Gray [71]. He explained this tendency for N-I transitions using the structure of the alkyl chain. He explained the molecular

conformation of the alkyl chain, which is confirmed by X-ray investigations of the crystalline nature of several mesomorphic compounds.

The N-I transition temperatures will be influenced by the following factors as the chain length increases, with the impacts that prevail being as follows:

1. The longer molecules will find it more difficult to prolong the ordered state.
2. Every additional methylene unit results in an increase in overall polarizability.
3. In the fluid nematic melt, the frequency at which the molecules easily polarizable aromatic portions are positioned adjacent to one another will decrease.
4. Each methylene unit reduces the molecules remaining terminal attractions by forcing the polarizable centres apart.

Based on their analyses of the dipole moment and dielectric anisotropies of a nematogenic homologous series, Maier [75] and Maier and Baumgartner [74] have also attempted to explain the alternation effect. The odd-even phenomenon in isotropic-nematic transition temperatures and entropies is explained by Marcelja [70]. It has been demonstrated from the geometry of p,p'-di-n-alkoxy azoxybenzenes that the addition of carbon atom C2 improves the anisotropy of the molecule and facilitates the ordering process; the addition of atom C3, later on, hinders the ordering process, atom C4 again facilitates the ordering process, and so on. Because of the chains' flexibility, the effect gets weaker as they go longer and eventually disappear for long-end chains.

Pines *et al.* [76] determined the order parameters in a series of nematic liquid crystals p-alkoxyazoxybenzene. From the series, an odd-even shift in the regular pattern was observed. They attributed that for the complete series and throughout the nematic range, the benzene rings rotate or flip about the para axes at a rate greater than 1 kHz. In their analysis of various experimental findings about the fluctuation of the nematic-isotropic transition temperatures T_{N-I}, De Jeu and Van der Veen [77] assessed molecular structure using formulas for T_{N-I} derived from theories of molecular statistics.

The mesophases attributed in both prepared series-I and II were identified according to their microscopic textures. A polarising optical microscope was used to observe these textures. Using heating and cooling cycles, POM was used to determine the smectic and nematic phases based on textural images. The smectic phase has a broken focal conic or broken fan-shaped texture, which is typical of the smectic A type. A known SmA molecule can be mixed in to further confirm the Smectic A phase. A typical marble-like texture is evident during the nematic phase. Thermal microscopy phase transition temperatures were found to be reasonably

consistent with the related DSC thermograms. Microscopic images are represented in Figure 2.17.

2.3.1 Texture analysis of series-I and II [(4a-4l) and (5a-5l)]

In series-I, the lower homologue from **4a-4c**, when melted initially, exhibited a nematic phase with a typical marble-like texture which on further heating is converted into isotropic liquid. On cooling the sample, the nematogenic textures are observed which on further cooling at a certain temperature are converted into a crystalline compound. Marble droplets of nematic phase textures with four brush defects were observed in compound **4d** on heating at 137.2 °C (Figure 2.17(b)) The Cr-SmA transition of compound **4d** (Figure 2.18(b)) is seen, whereas the transition of the SmA-Nematic mesophase, associated with the small enthalpy change value was observed in the DSC thermogram (Figure 2.18(b)). A very minute curve representing the N-Iso transition (compound **4d**) was observed at 160 °C (Figure 2.18(b)). On cooling the sample, two small curves with minimal enthalpy change were observed at two different temperatures (159.1 °C and 137.1 °C) indicating the Iso-N and N-SmA transition. On further cooling, a sharp curve at 60 °C was seen in the DSC thermogram attributing to the SmA-Cr transition of compound **4d** (Figure 2.18(b)). The compounds **4d-4l**, on heating exhibit fan-shaped and focal conical textures of Smectic-A phases which on further heating, a typical marble-like texture of the nematic phase was observed. As it cools from the isotropic melt, the nematic textures were observed which on further cooling the sharp typical conical texture of Smectic-A phases was observed. Hence, an enantiotropic nature of all the proposed compounds was observed under the polarizing optical microscope.

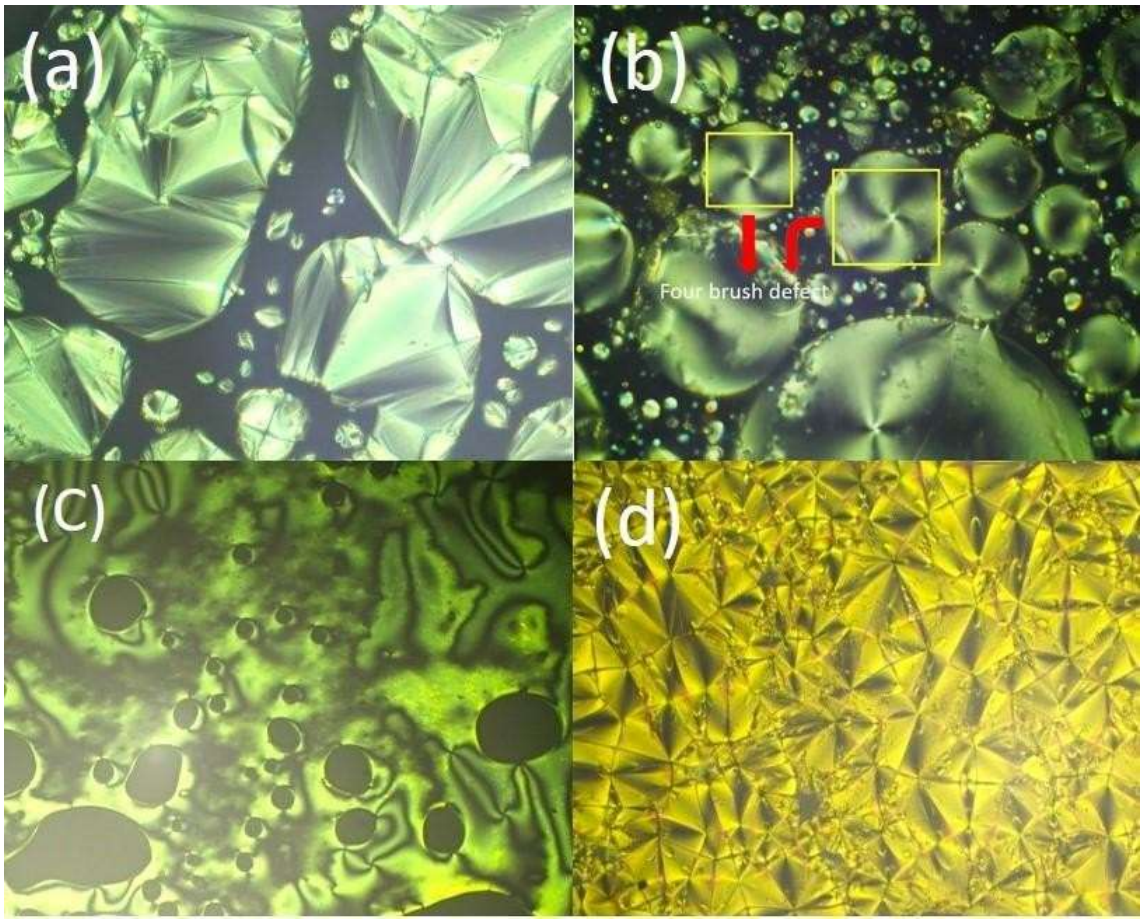

Figure 2.17: Microscopic textures were observed under POM for the different mesophases placed between two untreated glass slides. (a) The fan-shaped texture of Smectic A phase of compound **4d** on heating at 100.5 °C (b) Nematic phase with a typical marble texture of compound **4d** on heating at 137.2 °C (c) Nematic phase of compound **4d** on cooling at 158.2 °C (d) Typical Focal conic texture of a Smectic A phase of compound **4d** on cooling at 136.8 °C. All the microscopic textures were taken under the magnification of 10 X.

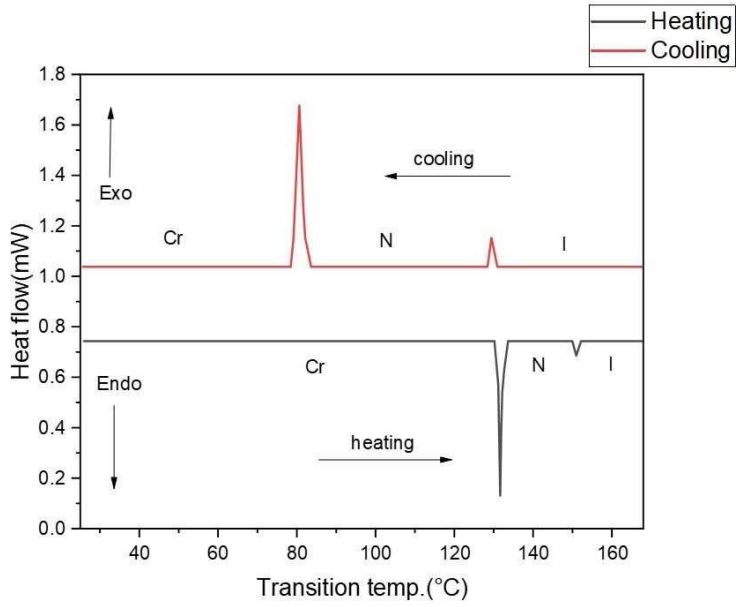

(a)

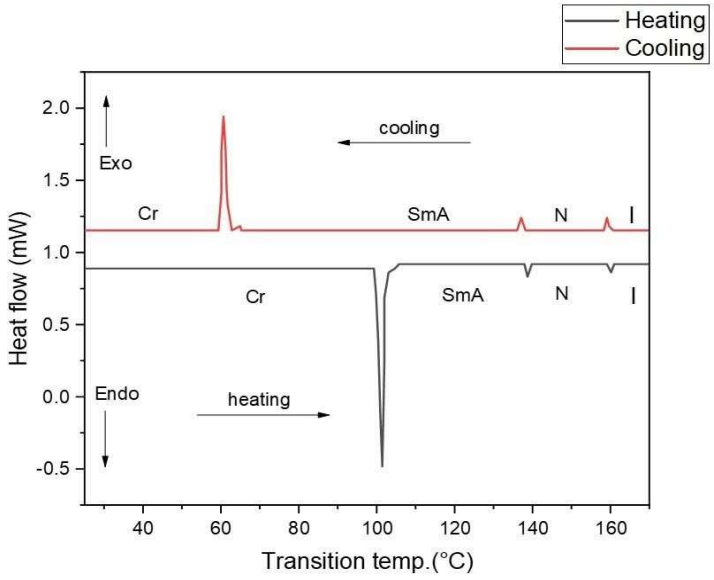

(b)

Figure 2.18: DSC thermogram of (a) compound **4c** and (b) compound **4d**

In series II, the lower homologue from **5a-5c** when melted initially exhibited a nematic phase with a typical marble-like texture which on further heating is converted into isotropic liquid. On cooling the sample, the nematogenic textures are observed which on further cooling at a certain temperature are converted into a crystalline compound. Marble droplets of nematic phase textures with four brush defects were observed in compound **5d** on heating at 114.5 °C.

The Cr-SmA transition of compound **5d** is observed, whereas the transition of the SmA-Nematic mesophase, associated with the small enthalpy change value was observed in the DSC thermogram. A very minute curve representing the N-Iso transition (compound **5d**) was observed at 158.2 °C. On cooling the sample, two small curves with minimal enthalpy change were observed at two different temperatures (155.2 °C and 112.4 °C) indicating the Iso-N and N-SmA transition. On further cooling, a sharp curve at 98.3 °C was observed in the DSC thermogram attributing to the SmA-Cr transition of compound **5d**. The compounds **5d-5l**, on heating exhibit fan-shaped and focal conical textures of Smectic-A phases which on further heating, a typical marble-like texture of the nematic phase was observed. As it cools from the isotropic melt, the nematic textures were observed which on further cooling the sharp typical conical texture of Smectic-A phases was observed. Hence, an enantiotropic nature of all the proposed compounds was observed under the polarizing optical microscope.

2.3.2 Thermal properties of series-I and II [(4a-4l) and (5a-5l)]

The transition temperature in °C, with transition enthalpy change (kJ mol^{-1}) values for compounds, **4a-4l** upon heating and cooling are listed in Table 2.3. Compounds **(4a-4b)** exhibited two peaks corresponding to crystal-nematic (Cr-N) and nematic-isotropic (N-Iso) with different transition enthalpy change values, confirming the enantiotropic mesophase. The stability of all the compounds was observed on repeated heating and cooling cycles. From the DSC thermogram of **4c** (Figure 2.18(a)), the endothermic peak was observed at 131.96 °C as an enthalpy change of 5.2 kJ/mol which is attributed to the Cr-N transition, and at 150 °C the nematic to isotropic transition is observed, one peak observed on cooling at 129.9 °C with ΔH = 1.73 kJ/mol attributed to Iso-N transition. This affirms that compound **4c** is purely a nematogen. Compound **4d** (Figure 2.17(b)) exhibits marble texture with four brush defects which confirms the presence of nematic ordering. In Figure 2.17(b,), on heating compound **4d** at 101.9 °C, an endotherm curve with corresponding phase transition change in enthalpy at 5.80 kJ/mol was observed indicating Crystal-SmA transition, and on further heating, another peak was observed at 138.1 °C with its enthalpy of 1.5 kJ/mol indicating SmA-N transition and on further heating a very small curve was observed at 160 °C indicating N-Iso transition. On cooling, exothermic curve at 159.1 °C and 137.1 °C with change in enthalpy of 1.1 and 1.8 kJ/mol, corresponding to the Iso-N, N-SmA transition to SmA-Cr formation at 60 °C. These

above data assess the confirmation of the enantiotropic nature of compound **4d**. As we ascend the series, **(4e-4l)** exhibits three endothermic and exothermic curves corresponding to Cr-SmA, SmA-N, and N-Iso transitions. All the compounds **(4a-4l)** exhibit enantiotropic mesophases in heating and cooling cycles at different phase transition enthalpy change values. Initially, during the Cr-N/Cr-SmA transition, the phase transition enthalpy change data are fairly predicted which were attributed in Table 2.3. On the other hand, the enthalpy change values for N-Iso/SmA-N are found smaller than predicted.

The transition temperature in °C, with transition enthalpy change (kJ mol^{-1}) values for compounds (**5a-5l)** upon heating and cooling, are listed in Table 2.5. Compounds **(5a-5c)** exhibited two peaks corresponding to crystal-nematic (Cr-N) and nematic-isotropic (N-Iso) with different transition enthalpy change values, confirming the enantiotropic mesophase. The stability of all the compounds was observed on repeated heating and cooling cycles. From the DSC thermogram of compound **5c,** the peak was observed at 130.8 °C with ΔH = 4.5 kJ/mol which is attributed to the Cr-N transition, and at 155.3 °C the nematic to isotropic transition is observed, one peak observed on cooling at 150.9 °C with ΔH = 1.73 kJ/mol attributed to Iso-N transition. This affirms that compound **5c** is purely a nematogen. Compound **5d** exhibits marble texture with four brush defects which confirms the presence of nematic ordering. From DSC data, on heating compound **5d** at 107.2 °C, an endotherm curve with corresponding phase transition change in enthalpy at 4.6 kJ/mol was observed on further heating, and another peak was observed at 115.2 °C with its enthalpy of 1.5 kJ/mol attributing to SmA-N transition, and on heating at 158.2 °C converted into isotropic liquid. On cooling, exothermic curve at 155.2 °C and 112.4 °C with change in enthalpy of 1.1 and 1.8 kJ/mol, corresponding to the Iso-N, N-SmA transition to SmA-Cr formation at 98.3 °C. These above data assess the confirmation of the enantiotropic nature of compound **5d**. As we ascend the series, compound **(5e-5l)** exhibits three endothermic and exothermic curves corresponding to Cr-SmA, SmA-N, and N-Iso transitions. All the compounds **(5a-5l)** exhibit enantiotropic mesophases in heating and cooling cycles at different phase transition enthalpy change values. Initially, during the Cr-N/Cr-SmA transition, the phase transition enthalpy change data are fairly predicted which were attributed in Table 2.5. On the other hand, the enthalpy change values for N-Iso/Sm-N are found smaller than predicted.

Table 2.2: Transition temperatures of compounds (4a-4l) taken on Polarizing Optical Microscope [Series-I]

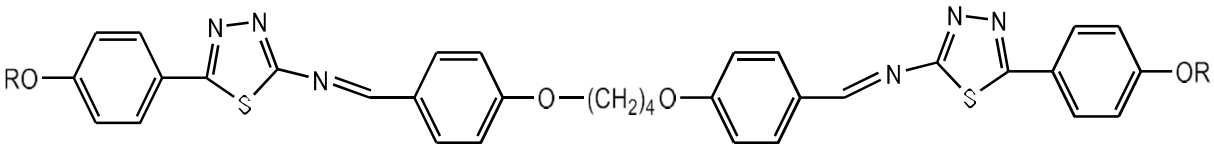

Sr. No.	Compound Code	R = n-alkyl group	Transition temperatures (°C)						
			Cr		SmA		N		I
1	4a	Methyl	•	-	•	101.5	•	184.4	•
2	4b	Ethyl	•	-	•	107.4	•	188.5	•
3	4c	Propyl	•	-	•	132.6	•	149.1	•
4	4d	Butyl	•	100.5	•	137.2	•	159.1	•
5	4e	Pentyl	•	121.5	•	134.9	•	154.4	•
6	4f	Hexyl	•	77.5	•	128.2	•	149.8	•
7	4g	Heptyl	•	87.1	•	128.9	•	146.6	•
8	4h	Octyl	•	85.5	•	127.5	•	148.1	•
9	4i	Decyl	•	86.5	•	128.5	•	147.6	•
10	4j	Dodecyl	•	89.7	•	127.4	•	141.5	•
11	4k	Tetradecyl	•	99.6	•	125.5	•	145.5	•
12	4l	Hexadecyl	•	123.5	•	124.3	•	149.4	•

Cr = crystal, SmA = smectic A, N = nematic, I = isotropic.

Table 2.3: Phase transition temperatures in °C along with transition enthalpy change (ΔH) (kJ mol-1) and for compounds 4a-4l a upon heating and cooling confirmed using Differential Scanning Calorimetry

Series Code	Heating (°C)	Cooling (°C)
4a	Cr 102.3 (4.9) N 185 (1.27) I	I 110.5 (4.8) N 86.4 (1.04) Cr
4b	Cr 108.4 (5.5) N 189.1 (1.08) I	I 112.7 (4.1) N 82.7 (1.23) Cr
4c	Cr 131.9 (5.2) N 150 (1.02) I	I 129.9 (1.73) N 80.0 (1.11) Cr
4d	Cr 101.9 (5.8) SmA 138.1 (1.5) N 160 (1.0) I	I 159.1 (1.1) N 137.1 (1.8) SmA 60 (2.1) Cr
4e	Cr 120.5 (5.9) SmA 133.2 (1.1) N 155 (1.2) I	I 154.0 (2.4) N 132.2 (1.9) SmA 67 (2.5) Cr
4f	Cr 78.8 (2.0) SmA 129.1 (1.0) N 150.9 (1.0) I	I 149.2 (1.5) N 128.5 (1.8) SmA 68.4 (3.3) Cr
4g	Cr 88.0 (1.5) SmA 127.1 (1.6) N 147.8 (1.0) I	I 146.2 (0.1) N 125.8 (1.2) SmA 60.3 (3.1) Cr
4h	Cr 86.6 (5.2) SmA 126.2 (1.1) N 147.1 (1.1) I	I 146.5 (1.3) N 125.8 (1.6) SmA 73.0 (3.6) Cr
4i	Cr 87.2 (5.9) SmA 129.1 (1.6) N 148.5 (1.2) I	I 146.0 (2.5) N 128.7 (1.3) SmA 71.4 (3.2) Cr
4j	Cr 90.3 (5.2) SmA 128.5 (1.9) N 142 (1.0) I	I 141.3 (1.5) N 126.4 (1.3) SmA 71.5 (2.8) Cr
4k	Cr 98.2 (5.3) SmA 126 (1.6) N 146 (1.0)I	I 145.8 (1.6) N 124.5 (1.4) SmA 78 (3.0) Cr
4l	Cr 124.5 (5.1) SmA 125 (1.1) N 150 (1.0) I	I 149.4 (1.5) N 123.3 (1.8) SmA 76 (3.5) Cr

Cr-crystalline solid, N-nematic mesophase, SmA-Smectic A mesophase, I-isotropic liquid

[a]Phase transition temperatures were noted by both Polarizing Optical Microscope and Differential Scanning Calorimetry studies: peak temperatures in the DSC thermograms obtained during the first heating and cooling cycles (scanning rate = 5 °C min^{-1}).

Table 2.4: Transition temperatures of compounds (5a-5l) taken on Polarizing Optical Microscope [Series-II]

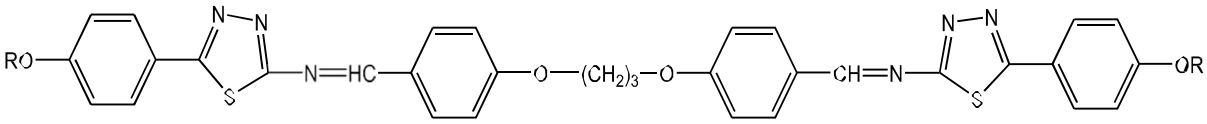

Sr. No.	Compound Code	R = n-alkyl group	Transition temperatures (°C)						
			Cr		SmA		N		I
1	5a	Methyl	•	-	•	103.1	•	187.7	•
2	5b	Ethyl	•	-	•	106.3	•	189.1	•
3	5c	Propyl	•	-	•	129.9	•	154.1	•
4	5d	Butyl	•	106.5	•	114.5	•	157.8	•
5	5e	Pentyl	•	102.5	•	131.5	•	154.4	•
6	5f	Hexyl	•	121.4	•	128.3	•	148.8	•
7	5g	Heptyl	•	79.5	•	125.5	•	145.5	•
8	5h	Octyl	•	86.5	•	126.1	•	144.8	•
9	5i	Decyl	•	86.1	•	129.1	•	146.5	•
10	5j	Dodecyl	•	85.5	•	129.1	•	143.5	•
11	5k	Tetradecyl	•	90.5	•	126.5	•	147.7	•
12	5l	Hexadecyl	•	100.3	•	125.5	•	149.6	•

Cr = crystal, SmA = smectic A, N = nematic, I = isotropic.

Table 2.5: Phase transition temperatures in °C along with transition enthalpy change (ΔH) (kJ mol-1) values for compounds 5a-5l a upon heating and cooling confirmed using Differential Scanning Calorimetry

Series Code	Heating (°C)	Cooling (°C)
5a	Cr 104.2 (4.2) N 188.1 (1.02) I	I 185.8 (4.8) N 90.2 (1.04) Cr
5b	Cr 107.4 (5.0) N 190.2 (1.01) I	I 178.4 (4.1) N 89.5 (1.23) Cr
5c	Cr 130.8 (4.5) N 155.3 (1.01) I	I 150.9 (1.73) N 91.1 (1.11) Cr
5d	Cr 107.2 (4.6) SmA 115.2 (1.5) N 158.2 (1.02) I	I 155.2 (1.1) N 112.4 (1.8) SmA 98.3 (2.1) Cr
5e	Cr 103.5 (4.9) SmA 132.1 (1.6) N 155.2 (1.05) I	I 153.4 (2.4) N 130.2 (1.9) SmA 100.2 (2.5) Cr
5f	Cr 122.5 (3.0) SmA 129.0 (1.2) N 149.8 (1.02) I	I 147.5 (1.5) N 127.5 (1.8) SmA 115.5 (3.3) Cr
5g	Cr 80.5 (1.2) SmA 126.1 (1.2) N 146.5 (1.01) I	I 144.2 (0.1) N 124.5 (1.2) SmA 75.4 (3.1) Cr
5h	Cr 87.6 (4.2) SmA 125.8 (1.0) N 145.2 (1.02) I	I 143.2 (1.3) N 123.4 (1.6) SmA 86.4 (3.6) Cr
5i	Cr 85.8 (3.9) SmA 130.1 (1.2) N 147.6 (1.0) I	I 145.5 (2.5) N 128.8 (1.3) SmA 84.5 (3.2) Cr
5j	Cr 86.8 (3.2) SmA 128.5 (1.0) N 144.5 (1.02) I	I 142.4 (1.5) N 127.5 (1.3) SmA 85.4 (2.8) Cr
5k	Cr 91.1 (3.3) SmA 127.0 (1.2) N 146.8 (1.01) I	I 145.6 (1.6) N 125.5 (1.4) SmA 90.2 (3.0) Cr
5l	Cr 101.8 (4.1) SmA 126.0 (1.0) N 150.5 (1.01) I	I 148.5 (1.5) N 125.2 (1.8) SmA 98.8 (3.5) Cr

Cr-crystalline solid, N-nematic mesophase, SmA-Smectic A mesophase, I-isotropic liquid

[a]Phase transition temperatures were noted by both Polarizing Optical Microscope and Differential Scanning Calorimetry studies: peak temperatures in the DSC thermograms obtained during the first heating and cooling cycles (scanning rate = 5 °C min^{-1}).

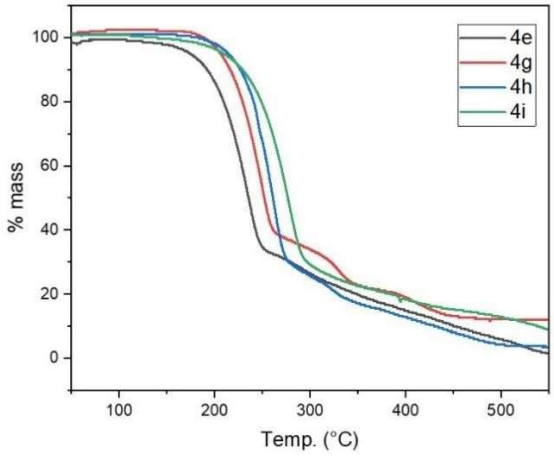

(a)

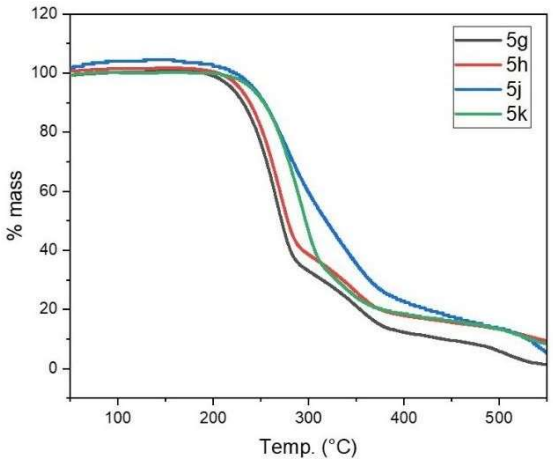

(b)

Figure 2.19: Representative thermogram of (a) 4e, 4g, 4h, 4i of series-I and (b) 5g, 5h, 5j, 5k of series-II was analyzed under a nitrogen atmosphere.

The TGA measurements of the compounds 4e, 4g, 4h, and 4i were performed in a temperature range from 50-550 °C in a nitrogen atmosphere. The TG curves of the compounds are illustrated in Figure 2.19. With the investigation of the mesogenic behavior of all the thiadiazole derivatives of series-I, it was observed that all the compounds were stable up to 180 °C attributing the thermal stability of prepared compounds. In series-II (Figure 2.19(b), it was observed that all the compounds were stable up to 200 °C.

2.3.3 Structure mesomorphic relationship

From the transition temperatures (°C**)** and transition enthalpy change values, it was observed that (**4a-4c**) derivatives lacks smectic phase, they only exhibit a pure nematic phase. In series-I, lower homologs are purely nematogens. The reason behind this is in the lower homologs, the aromatic nuclei separation was observed at a minimum level and the cohesions occurring at the terminal position are at the strongest level hence resulting in pure nematogens. Ascending the series, commencement in the smectic phase was observed in the middle members due to the dominance in the –OR group at the terminal position leading to the increasing lateral cohesive force resulting in the molecules alignment in the layer structure arrangement before entering the nematic phase. Hence, predominance in the smectogens was observed in the series. Figure 2.20(a) represents the mesogenic behaviour as a function of the number of carbon atoms in the

alkoxy chain for the transition temperature of the novel synthesized compounds. Lower chain compounds may result in stronger intermolecular attractions with an increase in transition temperature. On the contrary, higher chain compounds may enhance the flexibility of the molecule resulting in the lowering of the transition temperature. These above two factors (flexibility and intermolecular attractions) would contribute oppositely and predominate over each other in the case of medium alkoxy chain length and will decide the final transition temperature. In the crystal-mesophase transition, as we ascend the series the rising trend was observed till the n-propyl derivative (**4c**) followed by the odd-even effect till the n-octyl derivative (**4h**), with the increase in methylene unit, the increasing trend was observed till the compound **4l,** while in the smectic-nematic transition, with the rise in the alkoxy chain length at the terminal position, the characteristic decreasing tendency was observed upto n-octyl derivative (**4h**), an increasing trend was observed in compound **4i** followed by decreasing trend till compound **4l**. In the N-Iso transition, the alternate rising-falling tendency was observed till the n-pentyl derivative (**4e**), after that characteristic decrease in the trend was observed till compound 4h, followed by a falling-rising trend in transition temperature till compound **4l**.

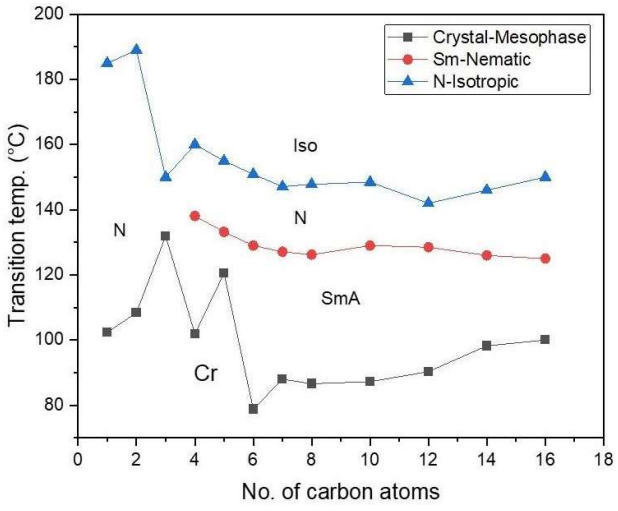

(a)

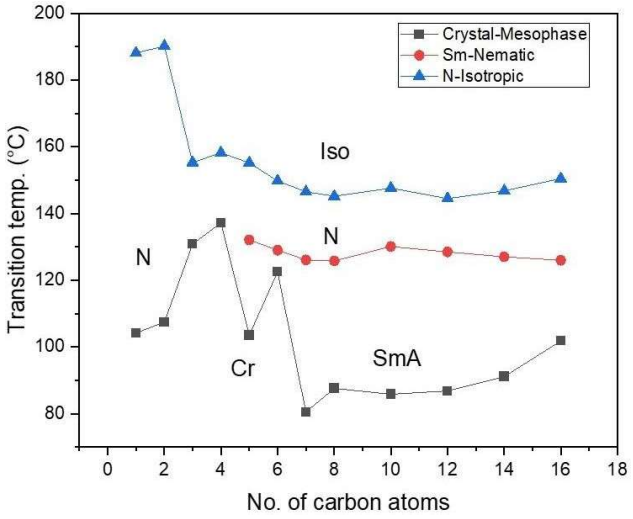

(b)

Figure 2.20: Variation of transition temperature with a number of carbon atoms in the alkoxy chain of the mesogenic compounds. (a) series-I, (b) series-II

In the crystal-mesophase transition (Figure 2.20(b)), as we ascend in the series-II, the rising trend was observed till the n-butyl derivative (**5d**) followed by the odd-even effect till the n-octyl derivative (**5h**), with the increase in methylene unit, the increasing trend was observed till the compound **5l,** while in the smectic-nematic transition, with the rise in the alkoxy chain length at the terminal position, the characteristic decreasing tendency was observed upto n-octyl derivative (**5h**), an increasing trend was observed in compound **5i** followed by decreasing trend till compound **5l**. In the N-Iso transition, the alternate rising-falling tendency was observed till the n-pentyl derivative (**5e**), after that characteristic decrease in the trend was observed till compound **5h**, followed by a falling-rising trend in transition temperature till compound **5l**.

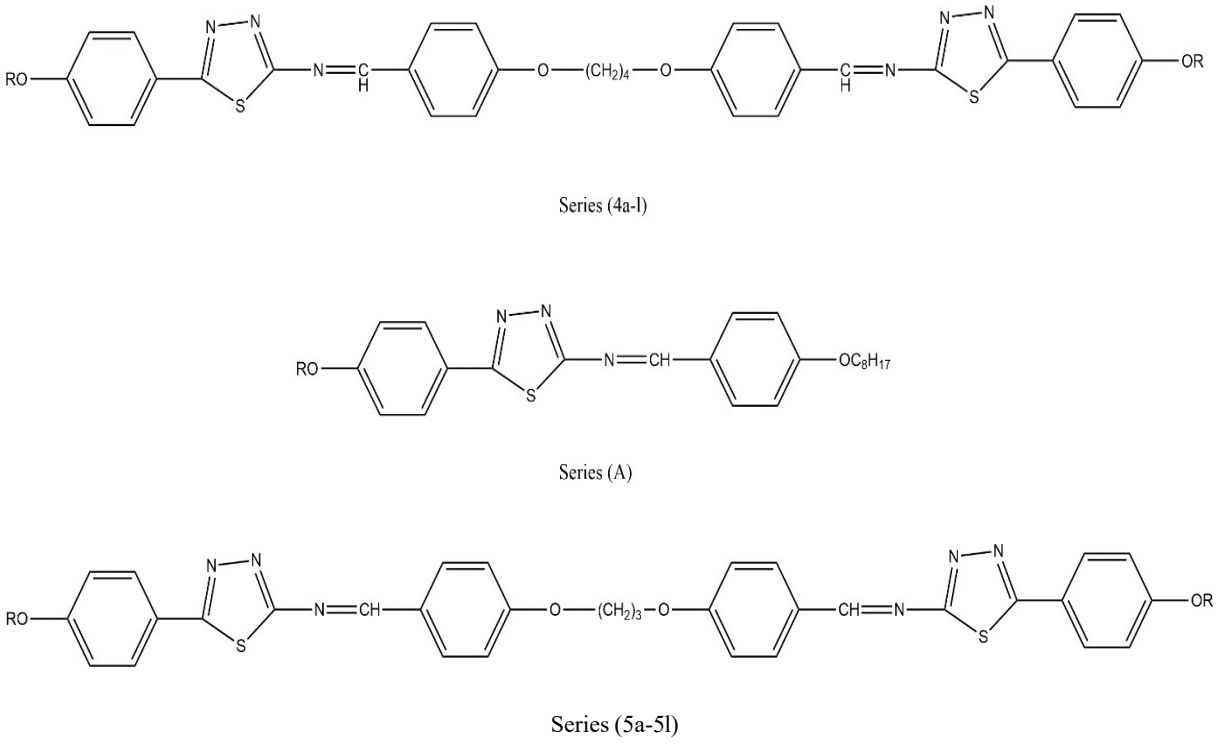

Figure 2.21: Comparison with novel synthesized compound

Comparison of newly prepared symmetrical homologous series-I and II with reported series:

1) 1,1'-((butan-1,4-diylbis(oxy))bis(4,1-phenylene))bis(*N*-5-(4-alkoxyphenyl)-1,3,4-thiadiazol-2-yl)methanimine); **Series-I**

2) 5-(4-n-alkoxy)-phenyl-2-(4-n-octyloxy) benzylidene-1,3,4-thiadiazoles; **Series (A)**

3) 1,1'-((propane-1,3-diylbis(oxy))bis(4,1-phenylene))bis(*N*-5-(4-alkoxyphenyl)-1,3,4-thiadiazol-2-yl)methanimine); **Series-II**

The average thermal stabilities of different mesomorphic homologous series are compared and recorded in Table 2.6.

Table 2.6: Average thermal stabilities of synthesized compounds with reported series

Series	I	II	A
N-Iso	148.5 (C_5-C_{10})	148.8 (C_5-C_{10})	204.9 (C_5-C_{10})
Sm-N	128.8 (C_5-C_{10})	128.6 (C_5-C_{10})	188.4 (C_5-C_{10})

Series-I and II contain 2-amino-5-(4'-alkoxyphenyl)-1,3,4-thiadiazole moiety attached with 1,4-bis (4'-formylphenoxy)alkane forming an azomethine linkage. Series **A** possesses only one Schiff's-base linkage at the core of the moiety. There are many factors such as molecular shape, intermolecular attractions, and packing skeleton that may influence the transition temperature of the mesogenic compounds. In **series-I** and **II**, the presence of the methylene unit in the central core of the moiety and the Schiff's-base attached at both sides to thiadiazole moiety leads to an increase in flexibility of the molecule with a concomitant influence in lowering the transition temperature and hence responsible for lowering the Sm-N and N-Isotropic thermal stability as compared to Series **A** compounds.

However, there is also another factor related to molecule shape that causes this change and causes the system to bend. This could also be explained by the thiadiazole core's higher molecular biaxiality. The liquid crystal compounds developed by Imrie *et al.* [78] have two mesogenic units divided by a flexible spacer. When in all trans-conformation, the typical behavior variations between odd- and even-membered compounds are typically described as the molecular shape's dependence on the spacer's parity.

Luckhurst *et al*. explained the variations in molecular geometry [79, 80]. The only two configurations that dimers can adopt were explained by Luckhurst *et al.* to comprehend how geometrical parameters affect the transitional features of dimers are bent and linear structures [81, 82].

It was observed that the transitional enthalpy change for the smectic A-nematic transition for homologue 7 is 1.6 kJ mole^{-1}, which is significantly less than the transitional enthalpy change for homologue 14. For homologue 14, the transitional enthalpy change is 1.9 kJ mole^{-1}. According to McMillan's theory, this is anticipated [83]. This hypothesis predicts that when the nematic phase length decreases, the enthalpy changes associated with the smectic-nematic

transition increases. In this case, homologue 14's molecular packing efficiency is probably greater than homologue 7's.

2.4. References

[1] Sugita SI, Toda S, Teraji T, Murayama A, Ishikawa M. Synthesis and Properties of Optically Active Phenoxypropionates Having Various Cores. Mol. Cryst. Liq. Cryst. 1993; **226**(1):7–12.

[2] Sugita SI, Toda S, Teraji T. Synthesis and Mesomorphic Properties of Ferroelectric Liquid Crystals Bearing 6-Phenyl-1,2,4-Triazine Rings. Mol. Cryst. Liq. Cryst. 1993; **237**(1):33–38.

[3] Lunkwitz R, Tschierske C, Langhoff A, Giebelmann F, Zugenmaier P. Axial Chiral Allenylacetates as Novel Ferroelectric Liquid Crystals. J. Mater. Chem. 1997; **7**(9):1713–1721.

[4] Schafer W, Rosenfeld U, Zaschke H, Stettin H, Kresse H. Preparation and Liquid Crystalline Properties of 1,3,4-thiadiazole derivatives. J. Prakt. Chem. 1989; **331**(4):631–636.

[5] Zab K, Joachimi D, Novotna E, Diele S, Tschierske C. Heterotrimeric Liquid Crystalline thiadiazole derivatives. Liq. Cryst. 1995; **18**(4):631–637.

[6] Bradley P, Sampson P, Seed AJ. Preliminary Communication: The synthesis of new mesogenic 1,3,4-thiadiazole-2-carboxylate esters via a novel ring closure. Liq. Cryst. Today. 2005; **14**(1):15-18.

[7] Parra M, Belmar M, Villouta S, Martinez R, Zuniga C, Zunza H. Schiff's bases: Synthesis and mesomorphic properties. Bol. Soc. Chil. Quim. 1995; **40**(1):175–182.

[8] Parra M, Belmar J, Zunza H, Zuniga C, Villouta S, Martinez R. Synthesis and mesomorphic properties of 5-(p-n-alkoxy)phenyl-2-(p-n-octyloxy)benzylideneamino-1,3,4-thiadiazole. J. Prakt. Chem. 1995; **337**(1):325–327.

[9] Parra M, Fuentes G, Vera V, Villouta SH, Hernandez S. Design of New V-Shaped Thermotropic Liquid Crystals containing Heterocyclic Moiety. Bol. Soc. Chil. Quim. 1995; **40(1)**:455–460.

[10] Parra M, Villouta S, Vera S, Belmar J, Zuniga C, Zunza H, Naturforsch Z. Synthesis of fluorinated liquid crystals. Chem. Sci. 1997; **52**(4):1533–1538.

[11] Mohd A and Kumar S. Synthesis and anti-inflammatory, analgesic, ulcerogenic, and lipid peroxidation activities of some new 2-[(2,6-dichloroanilino)phenyl]acetic acid derivatives. Eur. J. Med. Chem. 2004; **39**(6):535-545.

[12] Park YS, Kim D, Lee H, and Moon B. Donor-acceptor-donor –type liquid crystals with a pyridazine ring. Org. Lett. 2006; **8**(21):4699-4702.

[13] Zhang H, Shiino S, Shishido A, Kanazawa A, Tsutsumi O, Shiono T and Ikeda T. A Thiopene Liquid Crystal as a Novel л-Conjugated Dye for Photo Manipulation of Molecular Alignment. Adv. Mater. 2000; **12**(18):1336-1339.

[14] Girdziunaite D, Tshierske C, Novotna Z, and Kresse H. New mesogenic 1,3,4-oxadiazole derivatives. Liq. Cryst. 1991; **10**(3):397-407.

[15] Bezborodov VS, Petrov PF, and Lapanik VI. Lateral substitution in Nematic systems. Liq. Cryst. 1997; **20**(6):771-788.

[16] Parra M, Vergara J, Alderete J & Zuniga C. Synthesis and mesomorphic properties of esters derived from Schiff's bases containing 1,3,4-thiadiazole. Liq. Cryst. 2004; **31**(11):1531-1537.

[17] Parra M, Vergara J, Zuniga C, Soto E, Sierra T & Serrano JL. New chiral Schiff's bases with a 1,3,4-thiadiazole ring in the mesogenic core: synthesis, mesomorphic and ferroelectric properties. Liq. Cryst. 2005; **32**(4):457-462.

[18] Chiellini E. Structural and stereochemical isomerism effects in thermotropic liquid crystalline polymers. Nuovo Cimento D. 1990; **12**(1):1179-1193.

[19] Barclay GG, Ober CK. Liquid crystalline and rigid-rod networks. Prog. In Poly. Sci. 1993; **18**(5):899-945.

[20] Parra M, Saavedra CG, Hidalgo PI & Elgueta EY. Novel chiral liquid crystals based on amides and azo compounds derived from 2-amino-1,3,4-thiadiazoles: synthesis and mesomorphic properties. Liq. Cryst. 2008; **35**(1):55-64.

[21] Parra ML, Elgueta EY, Vergara JM & Sanchez AI. Columnar liquid crystals based on amino-1,3,4-thiadiazole derivatives. Liq. Cryst. 2012; **39**(8):917-925.

[22] Belmar J. New liquid crystals containing the benzothiazol unit: amides and azo compounds. Liq. Cryst. 1999; **26**(3):389-396.

[23] Dimitrowa K, Hauschild J, Zaschke H, and Shubert H. 1,3,4-thiadiazole: Biphenyl and terphenylanalogue1,3,4-thiadiazole. J. Prakt. Chem. 1980; **322**(6):933-944.

[24] Schafer W, Rosenfeld U, Zaschke H, Stettin H, and Kresse H. 1,3,4-thiadiazole mit Cyclohexanstrukturfragmenten. J. prakt. Chem. 1989; **331**(4):631-636.

[25] Belmar J. Synthesis and mesomorphic properties of 2,6-disubstituted derivatives of quinolone: amides and esters. Liq. Cryst. 1999; **26**(1):9-15.

[26] Karamysheva LA, Kovshev EJ, Pavluchenko AI, Roitman KV, Titov VV, Torgova T, Grebenkin SI. New heterocyclic liquid crystalline compounds. Mol. Cryst. Liq. Cryst. 1981; **67**(1):241-251.

[27] Yan Xu, Baolong L, Huibiao L, Zijian G, Zihou T & Zheng X. Liquid crystalline thiadiazole derivatives: new ferroelectric thiadiazole derivatives. Liq. Cryst. 2002; **29**(2):199-202.

[28] Han J, Wang JY, Zhang FY, Zhu LR, Pang ML & Meng JB. Synthesis and mesomorphic behavior of heterocycle-based liquid crystals containing 1,3,4-oxadiazole/thiadiazole and thiopene units. Liq. Cryst. 2008; **35**(10):1205-1214.

[29] Karamysheva LA, Kvshev EJ, Pavluvhenko AI, Roitman KV, Titov VVT, Torgova SI, and Grebenkin MF. New heterocyclic liquid crystalline compounds. Mol. Cryst. Liq. Cryst. 1981; **67**(1):241-249.

[30] Cai R, and Samulski ET. New thermotropic liquid crystals derived from thiopenes. Liq. Cryst. 1991; **9**(1):617-621.

[31] Lee CK, Kim JH, Choi EJ, Zin WC & Chien LC. Antiferroelectric liquid crystal from a banana-shaped achiral molecule. Liq. Cryst. 2001; **28**(12):1749-1754.

[32] Petrov VF. Nitrogen-containing fused heterocycles as the structural fragments in calamatic liquid crystal. Liq. Cryst. 2001; **28**(2):217-240.

[33] Parra M, Alderete J, Zuniga C, Gallardo H, Hidalgo P, Vergara J, and Hernandes S. Azo compounds and Schiff-bases derived from 5-(4-pyridyl)-2-amino-1,3,4-thiadiazole: synthesis, mesomorphic properties and structural study by semi-empirical calculations. Liq. Cryst. 2001; **28**(11):1659-1666.

[34] Parra M, Hernandes S, Alderete J, and Zuniga C. New Schiff's bases containing 1,3,4-thiadiazole and 1,3,4-oxadiazole units. Liq. Cryst. 2000; **27**(8):995-1000.

[35] Chandrasekhar S. Discotic Liquid Crystals: A brief review. Liq. Cryst. 1993; **14**(1):3-14.

[36] Umadevi S, Sadashiva BK. Banana-shaped mesogens: mesomorphic properties of seven-ring esters derived from 5-chlororesorcinol. Liq. Cryst. 2005; 32(3):287-297.

[37] Nair GG, Rao DSS, Prasad SK. et al. Electrooptic and Viewing Angle Characteristics of a Display Device Employing a Discotic Nematic Liquid Crystal. Mol Cryst Liq Cryst. 2003; **397**(1):245–252.

[38] Sato M & Ohta R. Liquid crystalline semirigid polyesters based on phenylstilbene analogues of 1,3,4-thiadiazole. Liq. Cryst. 2007; **34**(3):295-303.

[39] Han J, Wang Q, Wu J, and Zhu Li-R. Synthesis and liquid crystalline properties of H-shaped 1,3,4-thiadiazole dimers. Liq. Cryst. 2015; **42**(1):127-133.

[40] Zab K, Jaochimi D, Novotna E, Diele S & Carsten T. Heterotrimeric liquid crystalline thiadiazole derivatives. Liq. Cryst. 1995; **18**(4):631-637.

[41] Tomma J. Synthesis and study of the mesomorphic behaviour of some new 1,3,4-thiadiazoline derivatives. Liq. Cryst. 2023; **50**(6):998-1006.

[42] Mandle RJ, Stock N, Cowling SJ, et al. Condensation of free volume in structures of nematic and hexatic liquid crystals. Liq Cryst. 2019; **46**(1):114–123.

[43] Da Rosa RR, Tariq M, Weber CS, et al. Hybrid liquid crystals tetrazolyl and isoxazolyl cinnamates. Liq Cryst. 2016; **43**(1), 1659–1670.

[44] Chen BQ, Wen JX. Synthesis and mesophase behavior of mesogens bearing omega, alpha, alpha-trihydroperfluoroalkoxy end tails. Liq Cryst. 1999; **26**(2):1135–1140.

[45] Abberley JP, Killah R, Walker R, et al. Heliconical smectic phases formed by achiral molecules. Nat Commun. 2018; **9**(1):1-7.

[46] Paterson DA, Crawford CA, Pociecha D, et al. The role of a terminal chain in promoting the twist-bend nematic phase: the synthesis and characterization of the 1-(4-cyanobiphenyl-4′-yl)-6-(4-alkyloxyanilinebenzylidene-4′-oxy) hexanes. Liq Cryst. 2018; **45**(13-15):2341–2351.

[47] Hagar M, Ahmed H, Saad G. Synthesis and mesophase behavior of Schiff base/ester 4-(arylideneamino) phenyl-4 ″-alkoxy benzoates and their binary mixtures. J Mol Liq. 2019; **273**(1):266–273.

[48] Kornis GI. Comprehensive heterocyclic chemistry, five-membered rings with more than two heteroatoms and fused carbocyclic derivatives. Oxford: Elsevier Science; 1996.

[49] Loos-Wildenauer M, Kunz S, Voigt-Martin IG, Yakimanski A, Wischerhoff E, Zentel R, Tschierske C, Muller M. Second harmonic generation in ferroelectric liquid crystalline thiadiazole derivatives. Adv Mater. 1995; **7**(2):170–173.

[50] Parra M, Belmar J, Zunza H, Zuñiga C, Villouta S, Martinez R. Synthesis of amides derived from 1,3,4-thiadiazole as a mesogenic unit. Bol Soc Chil Quim. 1993; **38**(4):325–330.

[51] Parra M, Alderete J, Zúniga C, Hernandez S. Synthesis mesomorphic properties and structural study by semiempirical calculations of amides containing the 1,3,4-thiadiazole unit. Liq Cryst. 2002; **29**(5):647–652.

[52] Lai LL, Wang E. New synthesis of N,N-disubstituted (4-aminophenyl)diazenyl-1,3,4-thiadiazole, and mesogenic study and molecular modeling of its H-bonded complexes with a series of m-alkoxybenzoic acid derivatives. Helv Chim Acta. 2001; **84**(1):3581–3587.

[53] Xu Y, Zhu Z-G, Xu Z. Liquid crystalline thiadiazole derivatives: thiadiazole derivatives containing pyridine ring as a terminal group. Chin J Chem. 2001; **19**(9):870–876.

[54] Petrenko A, Goodby JW. V-shaped switching and interlayer interactions in ferroelectric liquid crystals. J Mater Chem. 2007; **17**(8):766–782.

[55] Sybo B, Bradley P, Grubb A, Miller S, Proctor KJW, Clowes L, Lawrie MR, Sampson P, Seed AJ. 1,3,4-Thiadiazole-2-carboxylate esters: a new synthetic methodology for the preparation of an elusive family of self-organizing materials. J Mater Chem. 2007; **17**(32): 3406–3411.

[56] Kolavi G, Hegde V, Khazi IA. Novel pyridazine fused heterocyclic system. A new route for the synthesis of 2-alkyl/aryl[1,3,4]thiadiazole[2′3′:2,3]imidazo[4,5-d]pyridazin-8(7H)-one. Synth Commun. 2006; **36**(13):1837–1843.

[57] Gallardo H, de Santos DMP, Caramori GF, Molin F, Bechtold IH. Synthetic pathway for a new series of liquid crystal 2,6-disubstituted imidazo[2,1-b[1,3,4]thiadiazole. Liq Cryst. 2013; **40**(5):570–580.

[58] Pati A, Patra M, Behera RK. Synthesis and spectral properties of macrocyclic compounds containing 1,3,4-thiadiazole moieties connected by a carbon-oxygen bridge. Synth Commun. 2006; **36**(12):1801–1808.

[59] Sato M, Matsuoka Y, Yamaguchi I. Bluish-violet light-emitting liquid crystalline hyperbranched polymers using three trisalcohol B3 monomers: Preparation, characterisation and structure-property relationship. Liq Cryst. 2012; **39**(9):1071–1081.

[60] Bradley P, Sampson P, Seed AJ. Preliminary communication: the synthesis of new mesogenic 1,3,4-thiadiazole-2-carboxylate esters via a novel ring closure. Liq Cryst Today. 2005; **14**(1):15–18.

[61] Yarovenko VN, Shirokov AV, Zavarzin IV, Krupinova ON, Igenatenko AV, Krayushkin MM. Synthesis of 4,5-dihydro-1,3,4-thiadiazole-2-carboxamide and 2-carbamoyl-4,5-dihydro-1,3,4-thiadiazole 1-oxide derivatives based on hydrazones of oxamic acid thiohydrazides. Chem Heterocycl. Compd. 2003; **39**(12):1633–1638.

[62] Kamotra P, Gupta AK, Gupta R, Somal P, Singh S. Microwave-assisted synthesis and biological activity of 3-alkyl/aryl-6-(1-chloro-3,4-dihydronaphth-2-yl)-5,6-dihydro-s-triazolo[3,4-b][1,3,4]thiadiazoles. Indian J Chem Sect B: Org Chem Incl Med Chem. 2007; **46B**(6):980–984.

[63] Han J, Chang X, Wang X, Zhu L, Pang M and Meng J. Microwave-assisted synthesis and liquid crystal properties of 1,3,4-thiadiazole derivatives based liquid crystals. Liq. Cryst. 2009; **36**(2):157-163.

[64] Han J, Zhang M, Wang F & Geng Q. Non-symmetric liquid crystal dimers based on 1,3,4-oxadiazole derivatives: synthesis, photoluminescence and liquid crystal behaviour. Liq. Cryst. 2010; **37**(12):1471-1478.

[65] Seltmann J and Lehmann M. Low-melting nematic V-shaped 1,3,4-thiadiazoles-phase engineering using small substituents and mixtures of flexible chains. Liq. Cryst. 2011; **38**(4), 407-422.

[66] Tan X, Zhang R, Guo C, Cheng X, Gao H, Liu F, Bruckner JR, Prehm M and Tschierske C. Amphoteric azobenzene derivatives with oligooxyethylene and glycerol based polar groups. J. Mat. Chem. C. 2015; **3**(1):11202-11211.

[67] Gray WBG, and Jones B. Mesomorphism and Chemical Constitution: The trans p-n-alkoxycinnamic acids. Journ. of the Chem. Soc. 1954; 1467-1470.

[68] Dave JS, and Vora RA, Molecular Crystals and Liquid Crystals. Mesomorphic behaviour of biphenyl Ester-I: Biphenyl-4-Trans-p-n-alkoxycinnamates. 1971; **14**(1):319-327.

[69] Greco C, and Ferrarini A. Entropy driven chiral order in a system of achiral bent particles. Phy. Rev. Lett. 2015; **115**(14):147801.

[70] Marcelja SJ. Chain ordering in Liquid Crystals: Structure of bilayer membranes. BBA-biomembranes. 1974; **367**(2):165-176.

[71] Gray GW. Comments on Some Recent Developments in the Field of Liquid Crystals. Mol. Cryst. and Liq. Cryst. 1981; **63**(1):3-17.

[72] Gray GW, and Goodby JW. Smectic F Phases Exhibited by the N-(4-N-Alkoxybenzylidene)-4'-n-Alkylanilines. 2011; **56**(2):43-49.

[73] Gray GW, and Goodby JW. Classification of Smectic Polymorphic Phases. 1979; **49**(7):217-223.

[74] Thaker BT et al. Synthesis, and characterization of liquid crystalline properties of Schiff's base ester central linkage involving 2,6-disubstituted naphthalene ring system. Liq. Cryst. 2012; **39**(5):1-19.

[75] Gray GW, and Goodby JW. Some New Smectic F Materials. 1978; **41**(6):145-150.

[76] Pines A, Ruben DJ, and Allison S. Molecular ordering and even-odd effect in a Homologous series of Nematic-Liquid Crystals. Phys. Rev. Lett.. 1974**; 33**(17):1002-1005.

[77] De Jeu WH and van der Veen J. Molecular Structure and Nematic Liquid Crystalline

Behaviour. Mol. Cryst. Liq. Cryst. 1977; **40**(1):1-17.

[78] Henderson PA, Niemeyer O and Imrie CT. Methylene Linked Liquid Crystal Dimers. Liq. Cryst. 2001; **28**(3):463-472.

[79] Emerson APJ and Luckhurst GR. On the relative propensities of ether and methyl linkages for liquid crystals formation in calamitics. Liq. Cryst. 1991; **10**(6):861-868.

[80] Ferrarini APJ, and Luckhurst GR. Prediction of the transitional properties of liquid crystals dimers. A molecular field calculation based on the surface tensor parametrization. J. Chem. Phys. 1994; **100**(2):1460-1469.

[81] Ferrarini A, Luckhurst GR, Nordio PL and Roskilly SJ. Understanding the unusual transitional behavior of liquid crystal dimers. Chem. Phys. Lett., 1993; **214**(3-4):409-417.

[82] Ferrarini A, Luckhurst GR, Nordio PL and Roskilly SJ. A shape model for molecular ordering in nematics. Liq. Cryst. 1996; **21**(3):373-382.

[83] McMillan WL. Simple Molecular Model for Smectic A phase of Liquid Crystals. Phys. Rev. A. 1971; **4**(3):1238-1246.